

## Respiratory Drive in Critically Ill Patients: Pathophysiology and Clinical Implications

Katerina Vaporidi<sup>1</sup>, Evangelia Akoumianaki<sup>1</sup>, Irene Telias<sup>2,3</sup>, Ewan C. Goligher<sup>2,4,5</sup>,  
Laurent Brochard<sup>2,3\*</sup>†, Dimitris Georgopoulos<sup>1\*</sup>

<sup>1</sup>Department of Intensive Care Medicine, University Hospital of Heraklion, Medical School University of Crete, Greece. <sup>2</sup>Interdepartmental Division of Critical Care Medicine, University of Toronto, Toronto, Canada. <sup>3</sup>Keenan Research Center and Li Ka Shing Knowledge Institute, St. Michael's Hospital, Toronto, Canada. <sup>4</sup>Department of Medicine, University Health Network, Toronto, Canada. <sup>5</sup>Toronto General Hospital Research Institute, Toronto, Canada

\*Equal contribution

† Deputy Editor, AJRCCM (participation complies with American Thoracic Society requirements for recusal from review and decisions for authored works).

Corresponding Author: D. Georgopoulos, Professor of Medicine,  
Director of Intensive Care Medicine Department,  
University Hospital of Heraklion, School of Medicine,  
University of Crete, Heraklion, Crete, Greece  
e-mail: georgopd@uoc.gr  
Phone: +306944727501

Author's contributions: D.G. and L.B. contributed to the conception of this work. K.V., E.A., I.T. and D.G. drafted and reviewed the manuscript. All authors critically revised the manuscript for intellectually important content and gave final approval of the version to be submitted.

All sources of support: none

Running head: Respiratory drive in critically ill patients

Descriptor number: 4.08

Word count: 5572

This article has an online data supplement, which is accessible from this issue's table of contents online at [www.atsjournals.org](http://www.atsjournals.org)

## Abstract

The respiratory drive, the intensity of the respiratory centers output, determines the effort exerted in each breath. The increasing awareness of the adverse effects of both strong and weak respiratory efforts during mechanical ventilation on patient outcome brings our attention to the respiratory drive of the critically ill patient. Critical illness can affect patients' respiratory drive through multiple pathways, mainly operating through three feedback systems: a) cortical, b) metabolic and c) chemical. The chemical feedback system, defined as the response of the respiratory center's output to changes in arterial blood gases and pH, is one of the most important determinants of respiratory drive. The purpose of this state-of-the-art review is to describe the determinants of respiratory drive in critically ill patients, review the tools available to assess respiratory drive at the bedside, and discuss the implications of altered respiratory drive during mechanical ventilation. An analysis that relates the arterial carbon dioxide levels with brain's response to this stimulus will be presented, contrasting the brain's responses to the patient's ability to generate effective alveolar ventilation, both during unassisted breathing and with different modes of ventilatory assist. This analysis may facilitate comprehension of the pathophysiology of respiratory drive in critically ill patients. As we aim to avoid both over- and under-assistance with mechanical ventilation, considering the patients' respiratory drive at the bedside may improve clinical assessment and management of the patient and the ventilator.

Word count: 232

Recent data indicate that during mechanical ventilation, both strong and weak respiratory efforts may adversely affect patient outcome through multiple pathways, such as patient-ventilator dyssynchrony, ventilation-induced lung injury (including patient-self-inflicted lung injury, P-SILI), diaphragmatic myotrauma, poor sleep quality, and cardiovascular compromise (1-6). It is important to recognize that the reason behind deleterious strong or weak respiratory efforts is a relatively high or low respiratory drive. In addition, the broad term “respiratory distress”, often described in critically ill patients as a reason for manipulating ventilation and sedation, implies high respiratory drive. It is therefore important for intensivists to recognize the determinants of respiratory drive in critically ill patients and, ideally, to assess the patient’s respiratory drive and effort when setting and managing mechanical assist. In this review we summarize the physiological control of respiratory drive and its determinants, and discuss the effects of critical illness and mechanical ventilation on respiratory drive. We then describe the methods available to evaluate respiratory drive at the bedside and discuss the clinical implications of altered respiratory drive in critically ill patients. We will focus on an analysis that relates CO<sub>2</sub> production and elimination with the brain’s response to this stimulus, contrasting this response to the patient’s ability to generate effective alveolar ventilation. This analysis aims to facilitate our understanding of how different variables modify respiratory drive in critically ill patients and to support clinical assessment and decision-making.

### **Respiratory Drive and the Inspiratory Flow-Generation Pathway**

Breathing is centrally controlled by the respiratory centers, a complex network of interconnected neurons in the medulla and pons. The respiratory centers receive rather constant (tonic) inputs from various sources which, through a complicated process, are

translated into an **output** with an **oscillatory pattern** (7-10). This **output** can be functionally divided into **rhythm-** and **pattern-generating signals** and **regulates** the **three phases** of the **respiratory cycle**: the **inspiratory**, **post-inspiratory**, and **expiratory** (7-11). The system employs '**gating**' to **modulate** the **inputs**, meaning that the **same tonic input** may have a **different effect** on the respiratory **centers** **depending** on the **phase** of the respiratory **cycle** (12). For example, a given input (i.e. PaCO<sub>2</sub>) activates the respiratory center during inspiration but **not** during expiration (Gate function, Figure 1).

During the inspiratory phase, the respiratory centers' output to the inspiratory muscles (electrical activity, EA<sub>brain</sub>) **gradually** rises, eventually reaching a **peak** value. Thereafter, the **post-inspiratory** phase begins and this output **subsides to the baseline value**. Finally, the **expiratory** phase commences, during which there is **no respiratory center activity** at resting breathing in healthy individuals. The **duration** of these three phases, although not always discrete, **determines** the **timing** of the **breath** and thus **breathing frequency**, whereas the **intensity** of the **output** is referred to as **respiratory drive** (7-10, 12-14). The **distinction** is **important** since respiratory **drive** **may change** **without** any **changes** in breath timing (i.e. **frequency**) and **vice versa** (15, 16).

The respiratory centers' output during the inspiratory phase travels through the **inspiratory flow-generation pathway** (Figure 1): from the **brainstem** and upper cervical spine neurons to the nucleus of **respiratory motoneurons**, leading to activation and contraction of the inspiratory muscles, finally resulting in the generation of inspiratory flow (7-9, 17-19).

In humans, since the **intensity of the respiratory centers' output**, cannot be directly **measured**, respiratory **drive** is **quantified** using the **average rate of increase of various indices of motor output** that, under certain circumstances, reflect the EA<sub>brain</sub>. Indeed, in healthy humans the respiratory drive determines the average rate of increase of (a) the

electrical activity of respiratory motoneurons (mainly the phrenic nerve in quiet breathing,  $dEA_{ph}/dt$ ), (b) the electrical activity of the diaphragm ( $dEA_{di}/dt$ ) and, during strenuous breathing of other inspiratory muscles, and c) the transdiaphragmatic pressure ( $dP_{di}/dt$ ), or pressure developed by all inspiratory muscles ( $dP_{mus}/dt$ ). Finally, the transdiaphragmatic pressure ( $P_{di}$ ) or  $P_{mus}$  is translated into flow ( $V'$ ) and volume ( $V$ ) according to the equation of motion (Figure 1) (19-21).

### **Determinants of Respiratory Drive**

The main inputs to the respiratory centers affecting the respiratory drive are the cortical and chemical feedback and the metabolic rate (7, 19, 20, 22). Reflex responses, such as the Hering-Breuer reflex affect mainly the duration of the inspiratory and expiratory phase of the breath (19, 23, 24). Cortical inputs may override the automatic control of breathing (i.e. voluntary apnea) (25, 26). In critically ill patients, sensory and emotional stimuli such as pain and anxiety, can significantly affect the respiratory drive (27, 28). Cortical inputs also mediate the effect of the wakefulness drive to breathe, as discussed below. Normally, in the absence of voluntary activity, the cerebral cortex exerts an inhibitory effect on the respiratory centers and decreases their output (29). High respiratory drive is common in critically ill patients with brain injury involving the cerebral cortex and is associated with poor outcome (30, 31). Although metabolic rate plays a key role in modulating the respiratory drive during exercise, linking  $CO_2$  production and elimination, its role in critically ill patients is unclear (32, 33). The main determinant of respiratory drive in many critically ill patients (and the most studied) is the chemical feedback, which is the response of the respiratory centers to changes in arterial blood gases and pH. Systemic inflammation and afferents from the lung and chest wall, through poorly described pathways, may also have a strong influence on the























this error (82, 92) but this method is cumbersome, relies on several assumptions, and is not suitable for every day clinical practice.

### C. Airway occlusion pressure ( $P_{0.1}$ )

Airway occlusion pressure or  $P_{0.1}$  is the drop in  $P_{aw}$  at the first 100 msec of an inspiratory effort against an occluded airway. The rationale to use it as an indicator of drive is that  $P_{0.1}$  increases proportionally to a rise in  $PaCO_2$  (21, 93) and during the short occlusion: 1)  $P_{aw}$  follows muscle pressure, 2) there is no significant behavioral or unconscious reaction, and 3) since no significant volume is displaced, abnormal respiratory mechanics do not affect the measurement. In healthy adults breathing at rest,  $P_{0.1}$  ranges between 0.5 to 1.5  $cmH_2O$ . In mechanically ventilated patients, values above 3.5  $cmH_2O$  have been associated with elevated respiratory muscle effort (esophageal pressure-time product greater than 200  $cm H_2O \cdot sec/min$ ) and indicate high drive (94).

$P_{0.1}$  is easily obtained in the ICU as it is an automated measurement available on the majority of modern ventilators (95), but some issues need to be considered to properly interpret  $P_{0.1}$  in critically ill patients. First,  $P_{0.1}$  could underestimate respiratory drive in very severe muscle weakness because of impairment in the inspiratory flow-generation pathway. In moderate-severe weakness, however,  $P_{0.1}$  still increases reliably with increasing  $PaCO_2$ , implying that the initial part of muscle contraction is relatively spared (54). Second, intrinsic positive end-expiratory pressure (PEEPi) can introduce a bias resulting from a phase lag between the change in  $P_{mus}$  and the change in  $P_{aw}$  during an occlusion. Nevertheless,  $P_{0.1}$  was shown to be a reasonable estimate of drive in intubated patients with PEEPi (96). Third, the decrease in  $P_{aw}$  at the beginning of a breath can result from relaxation of the expiratory muscles and the accuracy of  $P_{0.1}$  as a measure of drive in this condition is unknown (93). Fourth, the initial shape of the  $P_{mus}$ -

time curve may be influenced by increased resistance, exercise, or positive pressure ventilation, giving rise to some noise in the measurement (19, 97, 98). Fifth, breath-to-breath variability of  $P_{0.1}$  is significant, and the clinical measurement of  $P_{0.1}$  should be taken from an average of 3 to 4 measurements (99). Notwithstanding these pitfalls,  $P_{0.1}$  may provide indications of changes in drive.

#### **D. Clinical signs and breathing pattern**

Clinical signs of dyspnea and respiratory distress, whenever present, are good indicators of high drive, as dyspnea is directly linked to high drive (100, 101). A rapid shallow breathing pattern, the use of accessory inspiratory muscles, activation of expiratory muscles, tachycardia, hypertension, and diaphoresis have been associated with high respiratory drive (76, 101). Obviously, in patients with severe neuromuscular disease or cervical spine injury clinical signs of dyspnea may be blunted, as patients may not be able to recruit expiratory muscles or accessory inspiratory muscles, even in the presence of high respiratory drive.

Importantly, although it is generally accepted that tachypnea is an indicator of high drive and bradypnea of low drive, respiratory rate is a highly insensitive sign of increasing respiratory drive (2, 102). Even under normal conditions, respiratory rate has a rather large variability in between and within subjects. Moreover, respiratory rate changes little with changes in respiratory drive or ventilator support, until drive increases by more than 3-4 fold of resting value (2, 36, 38, 42-45).

#### **Clinical Implications**

Although respiratory drive may not be easily measured in the critically ill patient, and thresholds defining injurious high or low drive have not been defined, the clinical









## References

1. Talias I, Brochard L, Goligher EC. Is my patient's respiratory drive (too) high? *Intensive Care Med* 2018; 44: 1936-1939.
2. Akoumianaki E, Vaporidi K, Georgopoulos D. The Injurious Effects of Elevated or Nonelevated Respiratory Rate during Mechanical Ventilation. *Am J Respir Crit Care Med* 2019; 199: 149-157.
3. Goligher EC, Fan E, Herridge MS, Murray A, Vorona S, Brace D, Rittayamai N, Lanys A, Tomlinson G, Singh JM, Bolz SS, Rubenfeld GD, Kavanagh BP, Brochard LJ, Ferguson ND. Evolution of Diaphragm Thickness during Mechanical Ventilation. Impact of Inspiratory Effort. *Am J Respir Crit Care Med* 2015; 192: 1080-1088.
4. Goligher EC, Dres M, Fan E, Rubenfeld GD, Scales DC, Herridge MS, Vorona S, Sklar MC, Rittayamai N, Lanys A, Murray A, Brace D, Urrea C, Reid WD, Tomlinson G, Slutsky AS, Kavanagh BP, Brochard LJ, Ferguson ND. Mechanical Ventilation-induced Diaphragm Atrophy Strongly Impacts Clinical Outcomes. *Am J Respir Crit Care Med* 2018; 197: 204-213.
5. Brochard L. Ventilation-induced lung injury exists in spontaneously breathing patients with acute respiratory failure: Yes. *Intensive Care Med* 2017; 43: 250-252.
6. Hudson MB, Smuder AJ, Nelson WB, Bruells CS, Levine S, Powers SK. Both high level pressure support ventilation and controlled mechanical ventilation induce diaphragm dysfunction and atrophy. *Crit Care Med* 2012; 40: 1254-1260.
7. Del Negro CA, Funk GD, Feldman JL. Breathing matters. *Nat Rev Neurosci* 2018; 19: 351-367.
8. Richter DW, Smith JC. Respiratory rhythm generation in vivo. *Physiology (Bethesda)* 2014; 29: 58-71.
9. Guyenet PG, Bayliss DA. Neural Control of Breathing and CO<sub>2</sub> Homeostasis. *Neuron* 2015; 87: 946-961.
10. Ikeda K, Kawakami K, Onimaru H, Okada Y, Yokota S, Koshiya N, Oku Y, Iizuka M, Koizumi H. The respiratory control mechanisms in the brainstem and spinal cord: integrative views of the neuroanatomy and neurophysiology. *J Physiol Sci* 2017; 67: 45-62.
11. Agostoni E, Citterio G, D'Angelo E. Decay rate of inspiratory muscle pressure during expiration in man. *Respir Physiol* 1979; 36: 269-285.
12. Eldridge F.L. MDE. Oscillation, Gating, and Memory in the Respiratory Control System. *Comprehensive Physiology*; 2011. p. 93-114.

13. Mulkey DK, Stornetta RL, Weston MC, Simmons JR, Parker A, Bayliss DA, Guyenet PG. Respiratory control by ventral surface chemoreceptor neurons in rats. *Nat Neurosci* 2004; 7: 1360-1369.
14. Kam K, Worrell JW, Janczewski WA, Cui Y, Feldman JL. Distinct inspiratory rhythm and pattern generating mechanisms in the preBotzinger complex. *J Neurosci* 2013; 33: 9235-9245.
15. Corne S, Webster K, McGinn G, Walter S, Younes M. Medullary metastasis causing impairment of respiratory pressure output with intact respiratory rhythm. *Am J Respir Crit Care Med* 1999; 159: 315-320.
16. Costa R, Navalesi P, Cammarota G, Longhini F, Spinazzola G, Cipriani F, Ferrone G, Festa O, Antonelli M, Conti G. Remifentanyl effects on respiratory drive and timing during pressure support ventilation and neurally adjusted ventilatory assist. *Respir Physiol Neurobiol* 2017; 244: 10-16.
17. Zaki Ghali MG, Britz G, Lee KZ. Pre-phrenic interneurons: Characterization and role in phrenic pattern formation and respiratory recovery following spinal cord injury. *Respir Physiol Neurobiol* 2018.
18. Wu J, Capelli P, Bouvier J, Goulding M, Arber S, Fortin G. A V0 core neuronal circuit for inspiration. *Nat Commun* 2017; 8: 544.
19. Younes M. GD. Control of breathing relevant to mechanical ventilation. New York: Marcel Dekker; 1998. p. 1-74.
20. Tobin MJ, Laghi F, Jubran A. Ventilatory failure, ventilator support, and ventilator weaning. *Compr Physiol* 2012; 2: 2871-2921.
21. Whitelaw WA, Derenne JP, Milic-Emili J. Occlusion pressure as a measure of respiratory center output in conscious man. *Respir Physiol* 1975; 23: 181-199.
22. Mahamed S, Ali AF, Ho D, Wang B, Duffin J. The contribution of chemoreflex drives to resting breathing in man. *Exp Physiol* 2001; 86: 109-116.
23. Hamilton RD, Winning AJ, Horner RL, Guz A. The effect of lung inflation on breathing in man during wakefulness and sleep. *Respir Physiol* 1988; 73: 145-154.
24. Kondili E, Prinianakis G, Anastasaki M, Georgopoulos D. Acute effects of ventilator settings on respiratory motor output in patients with acute lung injury. *Intensive Care Med* 2001; 27: 1147-1157.
25. Mador MJ, Tobin MJ. Effect of alterations in mental activity on the breathing pattern in healthy subjects. *Am Rev Respir Dis* 1991; 144: 481-487.
26. Raux M, Straus C, Redolfi S, Morelot-Panzini C, Couturier A, Hug F, Similowski T. Electroencephalographic evidence for pre-motor cortex activation during inspiratory loading in humans. *J Physiol* 2007; 578: 569-578.

27. Tipton MJ, Harper A, Paton JFR, Costello JT. The human ventilatory response to stress: rate or depth? *J Physiol* 2017; 595: 5729-5752.
28. Raux M, Ray P, Prella M, Duguet A, Demoule A, Similowski T. Cerebral cortex activation during experimentally induced ventilator fighting in normal humans receiving noninvasive mechanical ventilation. *Anesthesiology* 2007; 107: 746-755.
29. Leitch AG, McLennan JE, Balkenhol S, McLaurin RL, Loudon RG. Ventilatory response to transient hyperoxia in head injury hyperventilation. *J Appl Physiol Respir Environ Exerc Physiol* 1980; 49: 52-58.
30. Esnault P, Roubin J, Cardinale M, D'Aranda E, Moncriol A, Cungi PJ, Goutorbe P, Joubert C, Dagain A, Meaudre E. Spontaneous Hyperventilation in Severe Traumatic Brain Injury: Incidence and Association with Poor Neurological Outcome. *Neurocrit Care* 2019; 30: 405-413.
31. Williamson CA, Sheehan KM, Tipirneni R, Roark CD, Pandey AS, Thompson BG, Rajajee V. The Association Between Spontaneous Hyperventilation, Delayed Cerebral Ischemia, and Poor Neurological Outcome in Patients with Subarachnoid Hemorrhage. *Neurocrit Care* 2015; 23: 330-338.
32. Haouzi P. Theories on the nature of the coupling between ventilation and gas exchange during exercise. *Respir Physiol Neurobiol* 2006; 151: 267-279.
33. Dempsey JA, Smith CA. Pathophysiology of human ventilatory control. *Eur Respir J* 2014; 44: 495-512.
34. Jacono FJ, Peng YJ, Nethery D, Faress JA, Lee Z, Kern JA, Prabhakar NR. Acute lung injury augments hypoxic ventilatory response in the absence of systemic hypoxemia. *J Appl Physiol (1985)* 2006; 101: 1795-1802.
35. Duffin J. The chemoreflex control of breathing and its measurement. *Can J Anaesth* 1990; 37: 933-942.
36. Duffin J, Mohan RM, Vasiliou P, Stephenson R, Mahamed S. A model of the chemoreflex control of breathing in humans: model parameters measurement. *Respir Physiol* 2000; 120: 13-26.
37. Rebuck AS, Slutsky AS. Measurement of ventilatory responses to hypercapnia and hypoxia. New York: Marcel Dekker; 1981. p. 745-772.
38. Patrick W, Webster K, Puddy A, Sanii R, Younes M. Respiratory response to CO<sub>2</sub> in the hypocapnic range in awake humans. *J Appl Physiol (1985)* 1995; 79: 2058-2068.
39. Skatrud JB, Dempsey JA. Interaction of sleep state and chemical stimuli in sustaining rhythmic ventilation. *J Appl Physiol Respir Environ Exerc Physiol* 1983; 55: 813-822.
40. Datta AK, Shea SA, Horner RL, Guz A. The influence of induced hypocapnia and sleep on the endogenous respiratory rhythm in humans. *J Physiol* 1991; 440: 17-33.

41. Meza S, Mendez M, Ostrowski M, Younes M. Susceptibility to periodic breathing with assisted ventilation during sleep in normal subjects. *J Appl Physiol (1985)* 1998; 85: 1929-1940.
42. Ranieri VM, Giuliani R, Mascia L, Grasso S, Petruzzelli V, Puntillo N, Perchiazzi G, Fiore T, Brienza A. Patient-ventilator interaction during acute hypercapnia: pressure-support vs. proportional-assist ventilation. *J Appl Physiol (1985)* 1996; 81: 426-436.
43. Scheid P, Lofaso F, Isabey D, Harf A. Respiratory response to inhaled CO<sub>2</sub> during positive inspiratory pressure in humans. *J Appl Physiol (1985)* 1994; 77: 876-882.
44. Georgopoulos D, Mitrouska I, Bshouty Z, Webster K, Patakas D, Younes M. Respiratory response to CO<sub>2</sub> during pressure-support ventilation in conscious normal humans. *Am J Respir Crit Care Med* 1997; 156: 146-154.
45. Xirouhaki N, Kondili E, Mitrouska I, Siafakas N, Georgopoulos D. Response of respiratory motor output to varying pressure in mechanically ventilated patients. *Eur Respir J* 1999; 14: 508-516.
46. Mitrouska J, Xirouchaki N, Patakas D, Siafakas N, Georgopoulos D. Effects of chemical feedback on respiratory motor and ventilatory output during different modes of assisted mechanical ventilation. *Eur Respir J* 1999; 13: 873-882.
47. Tobin MJ, Laghi F, Brochard L. Role of the respiratory muscles in acute respiratory failure of COPD: lessons from weaning failure. *J Appl Physiol (1985)* 2009; 107: 962-970.
48. Lopez-Barneo J, Gonzalez-Rodriguez P, Gao L, Fernandez-Aguera MC, Pardal R, Ortega-Saenz P. Oxygen sensing by the carotid body: mechanisms and role in adaptation to hypoxia. *Am J Physiol Cell Physiol* 2016; 310: C629-642.
49. Easton PA, Slykerman LJ, Anthonisen NR. Ventilatory response to sustained hypoxia in normal adults. *J Appl Physiol (1985)* 1986; 61: 906-911.
50. Duffin J. Measuring the ventilatory response to hypoxia. *J Physiol* 2007; 584: 285-293.
51. Volta CA, Alvisi V, Bertacchini S, Marangoni E, Ragazzi R, Verri M, Alvisi R. Acute effects of hyperoxemia on dyspnoea and respiratory variables during pressure support ventilation. *Intensive Care Med* 2006; 32: 223-229.
52. Aubier M, Murciano D, Fournier M, Milic-Emili J, Pariente R, Derenne JP. Central respiratory drive in acute respiratory failure of patients with chronic obstructive pulmonary disease. *Am Rev Respir Dis* 1980; 122: 191-199.
53. Doorduyn J, Nollet JL, Roesthuis LH, van Hees HW, Brochard LJ, Sinderby CA, van der Hoeven JG, Heunks LM. Partial Neuromuscular Blockade during Partial Ventilatory Support in Sedated Patients with High Tidal Volumes. *Am J Respir Crit Care Med* 2017; 195: 1033-1042.
54. Holle RH, Schoene RB, Pavlin EJ. Effect of respiratory muscle weakness on P<sub>0.1</sub> induced by partial curarization. *J Appl Physiol Respir Environ Exerc Physiol* 1984; 57: 1150-1157.

55. Borel CO, Teitelbaum JS, Hanley DF. Ventilatory drive and carbon dioxide response in ventilatory failure due to myasthenia gravis and Guillain-Barre syndrome. *Crit Care Med* 1993; 21: 1717-1726.
56. Moosavi SH, Topulos GP, Hafer A, Lansing RW, Adams L, Brown R, Banzett RB. Acute partial paralysis alters perceptions of air hunger, work and effort at constant P(CO<sub>2</sub>) and V(E). *Respir Physiol* 2000; 122: 45-60.
57. Mendonca CT, Schaeffer MR, Riley P, Jensen D. Physiological mechanisms of dyspnea during exercise with external thoracic restriction: role of increased neural respiratory drive. *J Appl Physiol (1985)* 2014; 116: 570-581.
58. Linton RA, Poole-Wilson PA, Davies RJ, Cameron IR. A comparison of the ventilatory response to carbon dioxide by steady-state and rebreathing methods during metabolic acidosis and alkalosis. *Clin Sci Mol Med* 1973; 45: 239-249.
59. Tojima H, Kunitomo F, Okita S, Yuguchi Y, Tatsumi K, Kimura H, Kuriyama T, Watanabe S, Honda Y. Difference in the effects of acetazolamide and ammonium chloride acidosis on ventilatory responses to CO<sub>2</sub> and hypoxia in humans. *Jpn J Physiol* 1986; 36: 511-521.
60. Javaheri S, Shore NS, Rose B, Kazemi H. Compensatory hypoventilation in metabolic alkalosis. *Chest* 1982; 81: 296-301.
61. Harper MH, Hickey RF, Cromwell TH, Linwood S. The magnitude and duration of respiratory depression produced by fentanyl and fentanyl plus droperidol in man. *J Pharmacol Exp Ther* 1976; 199: 464-468.
62. Akada S, Fagerlund MJ, Lindahl SG, Sakamoto A, Prabhakar NR, Eriksson LI. Pronounced depression by propofol on carotid body response to CO<sub>2</sub> and K<sup>+</sup>-induced carotid body activation. *Respir Physiol Neurobiol* 2008; 160: 284-288.
63. Pesenti A, Rossi N, Calori A, Foti G, Rossi GP. Effects of short-term oxygenation changes on acute lung injury patients undergoing pressure support ventilation. *Chest* 1993; 103: 1185-1189.
64. Hickmann CE, Roeseler J, Castanares-Zapatero D, Herrera EI, Mongodin A, Laterre PF. Energy expenditure in the critically ill performing early physical therapy. *Intensive Care Med* 2014; 40: 548-555.
65. Frank SM, Fleisher LA, Olson KF, Gorman RB, Higgins MS, Breslow MJ, Sitzmann JV, Beattie C. Multivariate determinants of early postoperative oxygen consumption in elderly patients. Effects of shivering, body temperature, and gender. *Anesthesiology* 1995; 83: 241-249.
66. Robertson CH, Jr., Foster GH, Johnson RL, Jr. The relationship of respiratory failure to the oxygen consumption of, lactate production by, and distribution of blood flow among

- respiratory muscles during increasing inspiratory resistance. *J Clin Invest* 1977; 59: 31-42.
67. Viale JP, Annat GJ, Bouffard YM, Delafosse BX, Bertrand OM, Motin JP. Oxygen cost of breathing in postoperative patients. Pressure support ventilation vs continuous positive airway pressure. *Chest* 1988; 93: 506-509.
68. Tappy L, Schwarz JM, Schneiter P, Cayeux C, Revelly JP, Fagerquist CK, Jequier E, Chiolero R. Effects of isoenergetic glucose-based or lipid-based parenteral nutrition on glucose metabolism, de novo lipogenesis, and respiratory gas exchanges in critically ill patients. *Crit Care Med* 1998; 26: 860-867.
69. Herve P, Simonneau G, Girard P, Cerrina J, Mathieu M, Duroux P. Hypercapnic acidosis induced by nutrition in mechanically ventilated patients: glucose versus fat. *Crit Care Med* 1985; 13: 537-540.
70. Manthous CA, Hall JB, Olson D, Singh M, Chatila W, Pohlman A, Kushner R, Schmidt GA, Wood LD. Effect of cooling on oxygen consumption in febrile critically ill patients. *Am J Respir Crit Care Med* 1995; 151: 10-14.
71. White DP, Weil JV, Zwillich CW. Metabolic rate and breathing during sleep. *J Appl Physiol (1985)* 1985; 59: 384-391.
72. Pestana D, Garcia-de-Lorenzo A, Madero R. Metabolic pattern and lipid oxidation during abdominal surgery: midazolam versus propofol. *Anesth Analg* 1996; 83: 837-843.
73. Kallet RH, Zhuo H, Liu KD, Calfee CS, Matthay MA, National Heart L, Blood Institute ANI. The association between physiologic dead-space fraction and mortality in subjects with ARDS enrolled in a prospective multi-center clinical trial. *Respir Care* 2014; 59: 1611-1618.
74. Lucangelo U, Blanch L. Dead space. *Intensive Care Med* 2004; 30: 576-579.
75. Sinha P, Flower O, Soni N. Deadspace ventilation: a waste of breath! *Intensive Care Med* 2011; 37: 735-746.
76. Jubran A. Rapid Shallow Breathing: Causes and Consequences. Berlin, Heidelberg: Springer; 2003. p. 161-168.
77. Kondili E, Prinianakis G, Georgopoulos D. Patient-ventilator interaction. *Br J Anaesth* 2003; 91: 106-119.
78. Goligher EC, Ferguson ND, Brochard LJ. Clinical challenges in mechanical ventilation. *Lancet* 2016; 387: 1856-1866.
79. Cinnella G, Conti G, Lofaso F, Lorino H, Harf A, Lemaire F, Brochard L. Effects of assisted ventilation on the work of breathing: volume-controlled versus pressure-controlled ventilation. *Am J Respir Crit Care Med* 1996; 153: 1025-1033.
80. Younes M. Proportional assist ventilation, a new approach to ventilatory support. Theory. *Am Rev Respir Dis* 1992; 145: 114-120.

81. Sinderby C, Navalesi P, Beck J, Skrobik Y, Comtois N, Friberg S, Gottfried SB, Lindstrom L. Neural control of mechanical ventilation in respiratory failure. *Nat Med* 1999; 5: 1433-1436.
82. Georgopoulos D, Mitrouska I, Webster K, Bshouty Z, Younes M. Effects of inspiratory muscle unloading on the response of respiratory motor output to CO<sub>2</sub>. *Am J Respir Crit Care Med* 1997; 155: 2000-2009.
83. Laghi F. Assessment of respiratory output in mechanically ventilated patients. *Respir Care Clin N Am* 2005; 11: 173-199.
84. Bellani G, Bronco A, Arrigoni Marocco S, Pozzi M, Sala V, Eronia N, Villa G, Foti G, Tagliabue G, Eger M, Pesenti A. Measurement of Diaphragmatic Electrical Activity by Surface Electromyography in Intubated Subjects and Its Relationship With Inspiratory Effort. *Respir Care* 2018; 63: 1341-1349.
85. Lin L, Guan L, Wu W, Chen R. Correlation of surface respiratory electromyography with esophageal diaphragm electromyography. *Respir Physiol Neurobiol* 2019; 259: 45-52.
86. Luo YM, Hart N, Mustfa N, Lyall RA, Polkey MI, Moxham J. Effect of diaphragm fatigue on neural respiratory drive. *J Appl Physiol (1985)* 2001; 90: 1691-1699.
87. Mauri T, Grasselli G, Suriano G, Eronia N, Spadaro S, Turrini C, Patroniti N, Bellani G, Pesenti A. Control of Respiratory Drive and Effort in Extracorporeal Membrane Oxygenation Patients Recovering from Severe Acute Respiratory Distress Syndrome. *Anesthesiology* 2016; 125: 159-167.
88. Beck J, Gottfried SB, Navalesi P, Skrobik Y, Comtois N, Rossini M, Sinderby C. Electrical activity of the diaphragm during pressure support ventilation in acute respiratory failure. *Am J Respir Crit Care Med* 2001; 164: 419-424.
89. Carreaux G, Cordoba-Izquierdo A, Lyazidi A, Heunks L, Thille AW, Brochard L. Comparison Between Neurally Adjusted Ventilatory Assist and Pressure Support Ventilation Levels in Terms of Respiratory Effort. *Crit Care Med* 2016; 44: 503-511.
90. Poulsen MK, Thomsen LP, Mifsud NL, Nielsen NP, Jorgensen RM, Kjaergaard S, Karbing DS. Electrical activity of the diaphragm during progressive cycling exercise in endurance-trained men. *Respir Physiol Neurobiol* 2015; 205: 77-83.
91. Corne S, Webster K, Younes M. Effects of inspiratory flow on diaphragmatic motor output in normal subjects. *J Appl Physiol (1985)* 2000; 89: 481-492.
92. American Thoracic Society/European Respiratory S. ATS/ERS Statement on respiratory muscle testing. *Am J Respir Crit Care Med* 2002; 166: 518-624.
93. Whitelaw WA, Derenne JP. Airway occlusion pressure. *J Appl Physiol (1985)* 1993; 74: 1475-1483.

94. Rittayamai N, Beloncle F, Goligher EC, Chen L, Mancebo J, Richard JM, Brochard L. Effect of inspiratory synchronization during pressure-controlled ventilation on lung distension and inspiratory effort. *Ann Intensive Care* 2017; 7: 100.
95. Telias I, Damiani F, Brochard L. The airway occlusion pressure (P0.1) to monitor respiratory drive during mechanical ventilation: increasing awareness of a not-so-new problem. *Intensive Care Med* 2018; 44: 1532-1535.
96. Conti G, Cinnella G, Barboni E, Lemaire F, Harf A, Brochard L. Estimation of occlusion pressure during assisted ventilation in patients with intrinsic PEEP. *Am J Respir Crit Care Med* 1996; 154: 907-912.
97. Gallagher CG, Younes M. Effect of pressure assist on ventilation and respiratory mechanics in heavy exercise. *J Appl Physiol (1985)* 1989; 66: 1824-1837.
98. Derenne JP, Whitelaw WA, Couture J, Milic-Emili J. Load compensation during positive pressure breathing in anesthetized man. *Respir Physiol* 1986; 65: 303-314.
99. Kera T, Aihara A, Inomata T. Reliability of airway occlusion pressure as an index of respiratory motor output. *Respir Care* 2013; 58: 845-849.
100. Faisal A, Alghamdi BJ, Ciavaglia CE, Elbehairy AF, Webb KA, Ora J, Neder JA, O'Donnell DE. Common Mechanisms of Dyspnea in Chronic Interstitial and Obstructive Lung Disorders. *Am J Respir Crit Care Med* 2016; 193: 299-309.
101. Parshall MB, Schwartzstein RM, Adams L, Banzett RB, Manning HL, Bourbeau J, Calverley PM, Gift AG, Harver A, Lareau SC, Mahler DA, Meek PM, O'Donnell DE, American Thoracic Society Committee on D. An official American Thoracic Society statement: update on the mechanisms, assessment, and management of dyspnea. *Am J Respir Crit Care Med* 2012; 185: 435-452.
102. Mauri T, Langer T, Zanella A, Grasselli G, Pesenti A. Extremely high transpulmonary pressure in a spontaneously breathing patient with early severe ARDS on ECMO. *Intensive Care Med* 2016; 42: 2101-2103.
103. Zambon M, Beccaria P, Matsuno J, Gemma M, Frati E, Colombo S, Cabrini L, Landoni G, Zangrillo A. Mechanical Ventilation and Diaphragmatic Atrophy in Critically Ill Patients: An Ultrasound Study. *Crit Care Med* 2016; 44: 1347-1352.
104. Vitacca M, Bianchi L, Zanotti E, Vianello A, Barbano L, Porta R, Clini E. Assessment of physiologic variables and subjective comfort under different levels of pressure support ventilation. *Chest* 2004; 126: 851-859.
105. Weinhouse GL, Schwab RJ, Watson PL, Patil N, Vaccaro B, Pandharipande P, Ely EW. Bench-to-bedside review: delirium in ICU patients - importance of sleep deprivation. *Crit Care* 2009; 13: 234.

106. Kim WY, Suh HJ, Hong SB, Koh Y, Lim CM. Diaphragm dysfunction assessed by ultrasonography: influence on weaning from mechanical ventilation. *Crit Care Med* 2011; 39: 2627-2630.
107. Jubran A, Tobin MJ. Pathophysiologic basis of acute respiratory distress in patients who fail a trial of weaning from mechanical ventilation. *Am J Respir Crit Care Med* 1997; 155: 906-915.
108. Tobin MJ, Perez W, Guenther SM, Semmes BJ, Mador MJ, Allen SJ, Lodato RF, Dantzker DR. The pattern of breathing during successful and unsuccessful trials of weaning from mechanical ventilation. *Am Rev Respir Dis* 1986; 134: 1111-1118.
109. Banzett RB, Lansing RW, Brown R, Topulos GP, Yager D, Steele SM, Londono B, Loring SH, Reid MB, Adams L, et al. 'Air hunger' from increased PCO<sub>2</sub> persists after complete neuromuscular block in humans. *Respir Physiol* 1990; 81: 1-17.
110. Yoshida T, Uchiyama A, Matsuura N, Mashimo T, Fujino Y. Spontaneous breathing during lung-protective ventilation in an experimental acute lung injury model: high transpulmonary pressure associated with strong spontaneous breathing effort may worsen lung injury. *Crit Care Med* 2012; 40: 1578-1585.
111. Yoshida T, Uchiyama A, Matsuura N, Mashimo T, Fujino Y. The comparison of spontaneous breathing and muscle paralysis in two different severities of experimental lung injury. *Crit Care Med* 2013; 41: 536-545.
112. Vaporidi K, Psarologakis C, Proklou A, Padiaditis E, Akoumianaki E, Koutsiana E, Chytas A, Chouvarda I, Kondili E, Georgopoulos D. Driving pressure during proportional assist ventilation: an observational study. *Ann Intensive Care* 2019; 9: 1.
113. Papazian L, Forel JM, Gacouin A, Penot-Ragon C, Perrin G, Loundou A, Jaber S, Arnal JM, Perez D, Seghboyan JM, Constantin JM, Courant P, Lefrant JY, Guerin C, Prat G, Morange S, Roch A, Investigators AS. Neuromuscular blockers in early acute respiratory distress syndrome. *N Engl J Med* 2010; 363: 1107-1116.
114. Yoshida T, Nakahashi S, Nakamura MAM, Koyama Y, Roldan R, Torsani V, De Santis RR, Gomes S, Uchiyama A, Amato MBP, Kavanagh BP, Fujino Y. Volume-controlled Ventilation Does Not Prevent Injurious Inflation during Spontaneous Effort. *Am J Respir Crit Care Med* 2017; 196: 590-601.
115. Mascheroni D, Kolobow T, Fumagalli R, Moretti MP, Chen V, Buckhold D. Acute respiratory failure following pharmacologically induced hyperventilation: an experimental animal study. *Intensive Care Med* 1988; 15: 8-14.
116. Roussos CS, Macklem PT. Diaphragmatic fatigue in man. *J Appl Physiol Respir Environ Exerc Physiol* 1977; 43: 189-197.
117. Aleksandrova NP, Isaev GG. Central and peripheral components of diaphragmatic fatigue during inspiratory resistive load in cats. *Acta Physiol Scand* 1997; 161: 355-360.

118. Ferguson GT. Respiratory failure due to altered central drive during inspiratory loading in rabbits. *Respir Physiol* 1995; 99: 75-87.
119. Bellemare F, Grassino A. Effect of pressure and timing of contraction on human diaphragm fatigue. *J Appl Physiol Respir Environ Exerc Physiol* 1982; 53: 1190-1195.
120. Vassilakopoulos T, Zakyntinos S, Roussos C. Respiratory muscles and weaning failure. *Eur Respir J* 1996; 9: 2383-2400.
121. Laghi F, Cattapan SE, Jubran A, Parthasarathy S, Warshawsky P, Choi YS, Tobin MJ. Is weaning failure caused by low-frequency fatigue of the diaphragm? *Am J Respir Crit Care Med* 2003; 167: 120-127.

## Figure Legends

**Figure 1: The Inspiratory flow-generation pathway.** Gate: the effects of afferent signals (inputs) vary depending on the phase of the inspiratory cycle they arrive; C3-C5: cervical spine levels;  $EA_{ph}$ ,  $dEA_{ph}/dt$ ,  $EA_{di}$ ,  $dEA_{di}/dt$ : electrical activity and change over time of the phrenic nerve, and diaphragm during inspiratory phase, respectively;  $P_{di}$ ,  $dP_{di}/dt$ : trasdiaphragmatic pressure and change over time during the inspiratory phase;  $V'$ : flow,  $\Delta V$ : volume above end-expiratory lung volume,  $R_{rs}$ ,  $E_{rs}$ : respiratory system resistance and elastance, respectively;  $P_{EE}$ : elastic recoil pressure at end-expiration (zero at functional residual capacity).  $dV/dt$ : change in volume over time;  $V_T/T_I$ : tidal volume to inspiratory time ratio or mean inspiratory flow.

**Figure 2:** Relationship between  $PaCO_2$  and minute ventilation obtained by the 1) graphical representation of the equation:  $PaCO_2 = 0.863 * V'CO_2 / [V'_E * (1 - V_D/V_T)]$ , the metabolic hyperbola (gray line), and 2) The  $PaCO_2$ -ventilation response curve (the change in minute ventilation induced by a change in  $PaCO_2$ ), during wakefulness (black solid line) and sleep (black dashed line) in a healthy subject. The intersection between the metabolic hyperbola and the ventilation curve defines  $PaCO_2$  at steady state during wakefulness and sleep (open and closed circles, respectively). Voluntary hyper- or hypo-ventilation could change  $PaCO_2$  anywhere along the metabolic hyperbola (white squares).  $V'_E$ : minute ventilation (l/min),  $V'CO_2$ :  $CO_2$  production (ml/min),  $V_D/V_T$ : dead space to tidal volume ratio.

**Figure 3:** Changes in minute ventilation (upper panel), tidal volume (middle panel) and breathing frequency (lower panel) versus end-tidal  $PCO_2$ , obtained from healthy young volunteers by a  $CO_2$ -rebreathing test. Notice the two different slopes of ventilation increase (S1 and S2) and the corresponding change in slope in tidal volume and respiratory rate increase (T1 and T2 mark the breakpoints separating the three segments

of different slope). In this subject, and in 75% of the examined cases, breathing frequency increased significantly when minute ventilation (ventilatory demands) was several-fold higher than basal ventilation. On the contrary tidal volume (and thus effort per breath, proportional to respiratory drive) increased significantly when  $\text{PCO}_2$  exceeded normal. From ref. 36 with permission.

**Figure 4:** A: Graphical representation of the metabolic hyperbola and brain/ventilation curve of a healthy human. The intersection of the metabolic hyperbola and ventilation curve (open circle) determines the steady-state  $\text{PaCO}_2$  and minute ventilation ( $V'_E$ ), 40 mmHg and 6.2 L/min, respectively (please note that these mathematically described curves and relationships are simplified presentations of experimental data, aiming to facilitate understanding of the effects of critical illness and mechanical ventilation on respiratory drive, and cannot be directly applied to compute the ventilatory demands of a critically ill patient).

B: This human develops severe pneumonia, causing increased  $\text{CO}_2$  production ( $V'\text{CO}_2$ ) and dead space to tidal volume ratio ( $V_D/V_T$ ) which move the metabolic hyperbola upward, and hypoxemia, which moves the brain curve to the left and increases its slope. Due to increased  $E_{rs}$ , a given respiratory centers output per minute (RCO/min) results in a lower  $V'_E$ , thus the slope of the ventilation curve is shifted downwards. A dissociation of the ventilation curve from the brain curve occurs. In the presence of a dissociation, any change in  $\text{PaCO}_2$  alters the RCO/min (mainly due to change in respiratory drive, RCO per breath), as much as the brain curve dictates, and any change in RCO/min can only change the actual ventilation as much as the ventilation curve dictates. Assuming for simplicity that the change in  $E_{rs}$ , and thus the deviation of ventilation curve, occurs abruptly, the RCO/min corresponds initially to point 1 ( $V'_E$  17.5 l/min), whereas the actual  $V'_E$  drops to point 2 (4.5 l/min). This decrease in ventilation leads to a gradual

increase of  $\text{PaCO}_2$ , which in turn stimulates the respiratory center. The  $\text{RCO}/\text{min}$  progressively increases along the brain curve (from point 1 to 3), following the increase in  $\text{PaCO}_2$ . In parallel, this increase in  $\text{RCO}/\text{min}$  results in an increase in the actual  $\text{V}'_{\text{E}}$  along the ventilation curve (from point 2 to 4). When  $\text{RCO}/\text{min}$  (point 3) results in an actual  $\text{V}'_{\text{E}}$  at intersection of the ventilation curve and metabolic hyperbola (point 4) a steady state occurs,  $\text{PaCO}_2$  stabilizes, and respiratory drive,  $\text{RCO}/\text{min}$  and  $\text{V}'_{\text{E}}$  do not increase further. Although brain's ventilation demands (46 L/min) are not met (actual  $\text{V}'_{\text{E}}=13$  L/min) respiratory drive and  $\text{RCO}/\text{min}$  do not increase further, since the  $\text{CO}_2$  stimulus is constant.

**Figure 5:** Metabolic hyperbola shifts from changes in dead space to tidal volume ratio ( $\text{V}_D/\text{V}_T$ ) and  $\text{CO}_2$  production ( $\text{V}'\text{CO}_2$ ). Vertical dotted lines indicate the different  $\text{PaCO}_2$  which would result if ventilation was the same (10 L/min) in all cases. Horizontal dotted lines indicate the different minute ventilation required to maintain the same  $\text{PCO}_2$  (40 mmHg) in all cases.

**Figure 6:** Effects of different modes of assisted mechanical ventilation on the ventilation curve and respiratory drive in a sedated patient in whom the un-assisted ventilation curve (black solid line) deviates from brain curve (black dashed line). For simplicity, metabolic hyperbola (gray line) and respiratory rate are constant in all conditions. Apneic threshold is set at  $\text{PaCO}_2$  of 35 mmHg. In each mode two levels of assist are shown (low and high, red lines). With all modes at low levels of assist, steady state occurs (open circles) while  $\text{PaCO}_2$  is lower than the  $\text{PaCO}_2$  during un-assisted breathing (intersection between un-assisted ventilation curve and metabolic hyperbola), but higher than the  $\text{PaCO}_2$  desired by the brain (intersection between brain curve and metabolic hyperbola). The respiratory center output ( $\text{RCO}/\text{min}$ ) is determined by the brain curve, at this  $\text{PaCO}_2$  (dark circle). At high level of assist the intersection between ventilation curve and metabolic hyperbola is

at lower  $\text{PaCO}_2$  than that desired by the brain. With assist-volume (A) and pressure support (B) a non-steady state occurs in this example, since the intersection of the metabolic hyperbola and the ventilation curve (open squares) is at a  $\text{PaCO}_2$  lower than the apneic threshold, respiratory drive hovers around zero, and the occurrence of apneas maintains  $\text{PaCO}_2$  close to apneic threshold (black squares). With proportional modes (C) even at highest assist (slope almost  $90^\circ$ ) a steady state is achieved (open circle) and  $\text{RCO}/\text{min}$  and respiratory drive although low, are always above zero (dark circle).

**Table 1: Conditions affecting the position of the brain and ventilation curve, and the metabolic hyperbola**

| <b>Brain curve</b>         | <b>Upwards/Left shift</b>   | <b>Downwards/right shift</b>   |
|----------------------------|---|--|
|                            | Metabolic acidosis  | Metabolic alkalosis  |
|                            | Hypoxemia   | Hyperoxemia  |
|                            | Interstitial lung edema   | Sedation   |
|                            | Brain pathology (cortical)  | Brain pathology (brain stem)   |
| <b>Ventilation curve</b>   | <b>Upwards/Left shift</b>   | <b>Downwards/right shift</b>   |
|                            | Mechanical ventilation  | Upper motor neuron disease   |
|                            | Partial or full recovery from diseases that affects Inspiratory-flow generation pathway (upward shift from disease state, towards normal) | Diseases affecting nerve conduction (Guillain-Barre)   |
|                            |   | Diseases affecting neuromuscular junction (myasthenia Gravis)                                  |
|                            |   | Respiratory muscle weakness/injury   |
|                            |   | Impaired diaphragm length-tension relationship   |
|                            |   | Increased airway resistance  |
|                            |   | Decreased respiratory system compliance  |
| <b>Metabolic Hyperbola</b> | <b>Upwards shift<br/>Increased <math>V_D/V_T</math>,<br/>Increased <math>V'CO_2</math></b>  | <b>Downwards shift<br/>Decreased <math>V_D/V_T</math> or<br/>Decreased <math>V'CO_2</math></b> |
|                            | Low tidal volume ( $V_D/V_T$ )  | High tidal volume ( $V_D/V_T$ )  |
|                            | Rapid shallow breathing ( $V_D/V_T$ )   | Sedation ( $V'CO_2$ )  |
|                            | Increased dead space - lung pathology ( $V_D/V_T$ )   | Hypothermia ( $V'CO_2$ )   |
|                            | Increased dead space – ventilator circuit ( $V_D/V_T$ )   |  |
|                            | Agitation/ shivering ( $V'CO_2$ )   |  |
|                            | Fever ( $V'CO_2$ )  |  |
|                            | Strenuous breathing ( $V'CO_2$ )  |  |

$V_D/V_T$ : dead space to tidal volume ratio,  $V'CO_2$ :  $CO_2$  production.

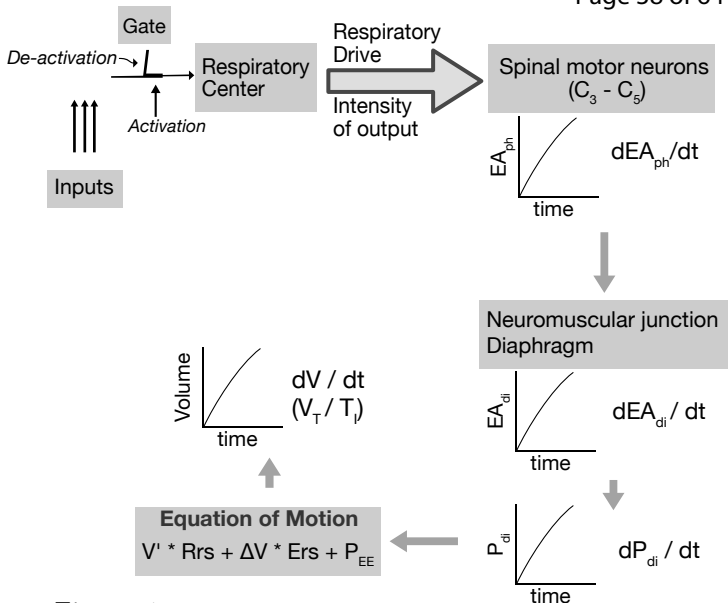


Figure 1

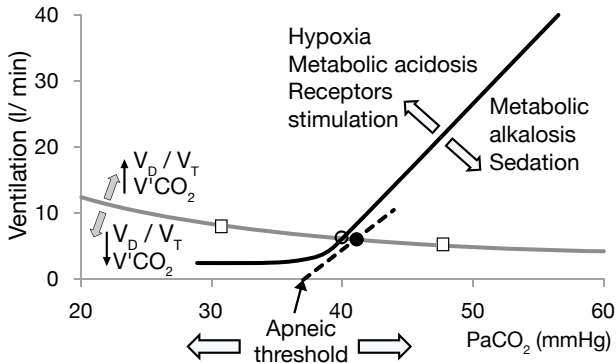


Figure 2

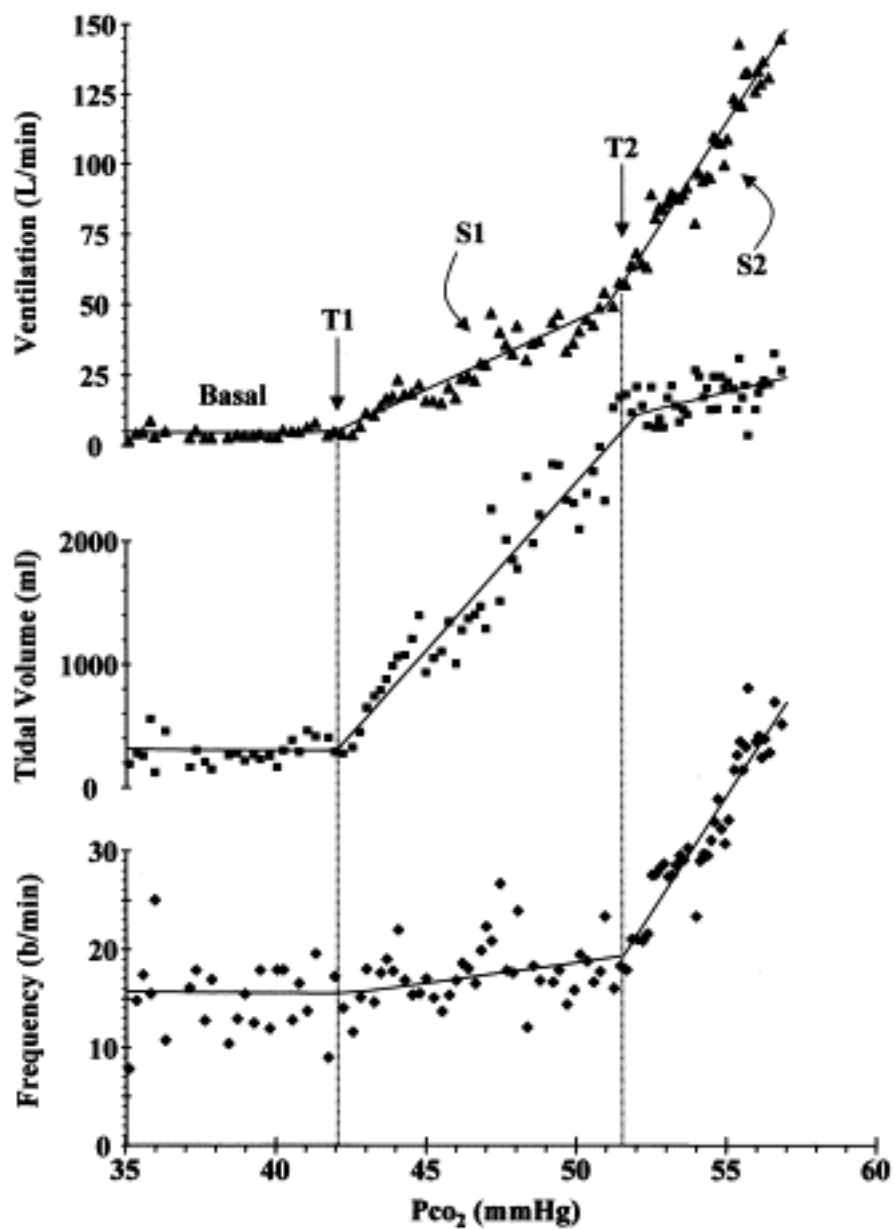


Figure 3

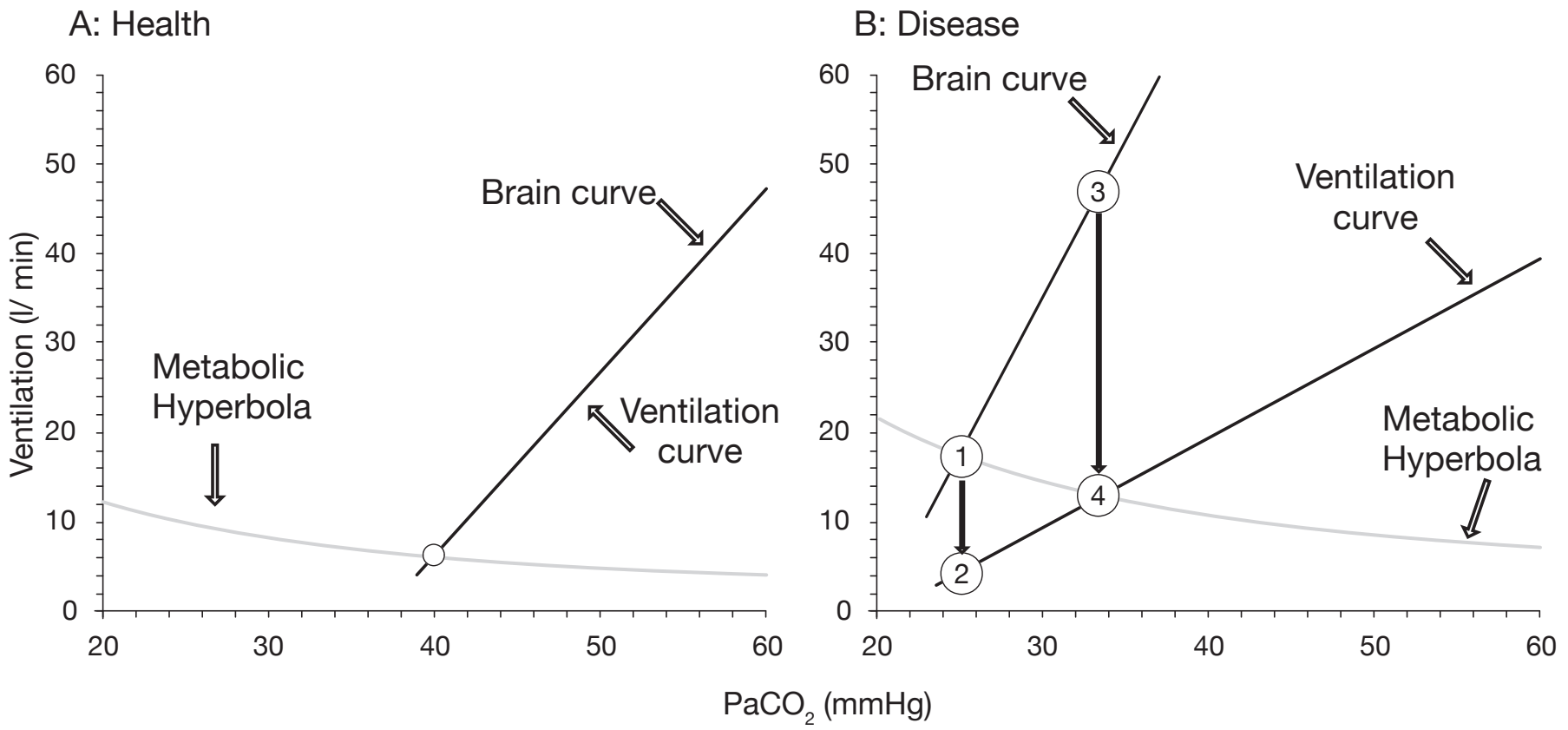


Figure 4

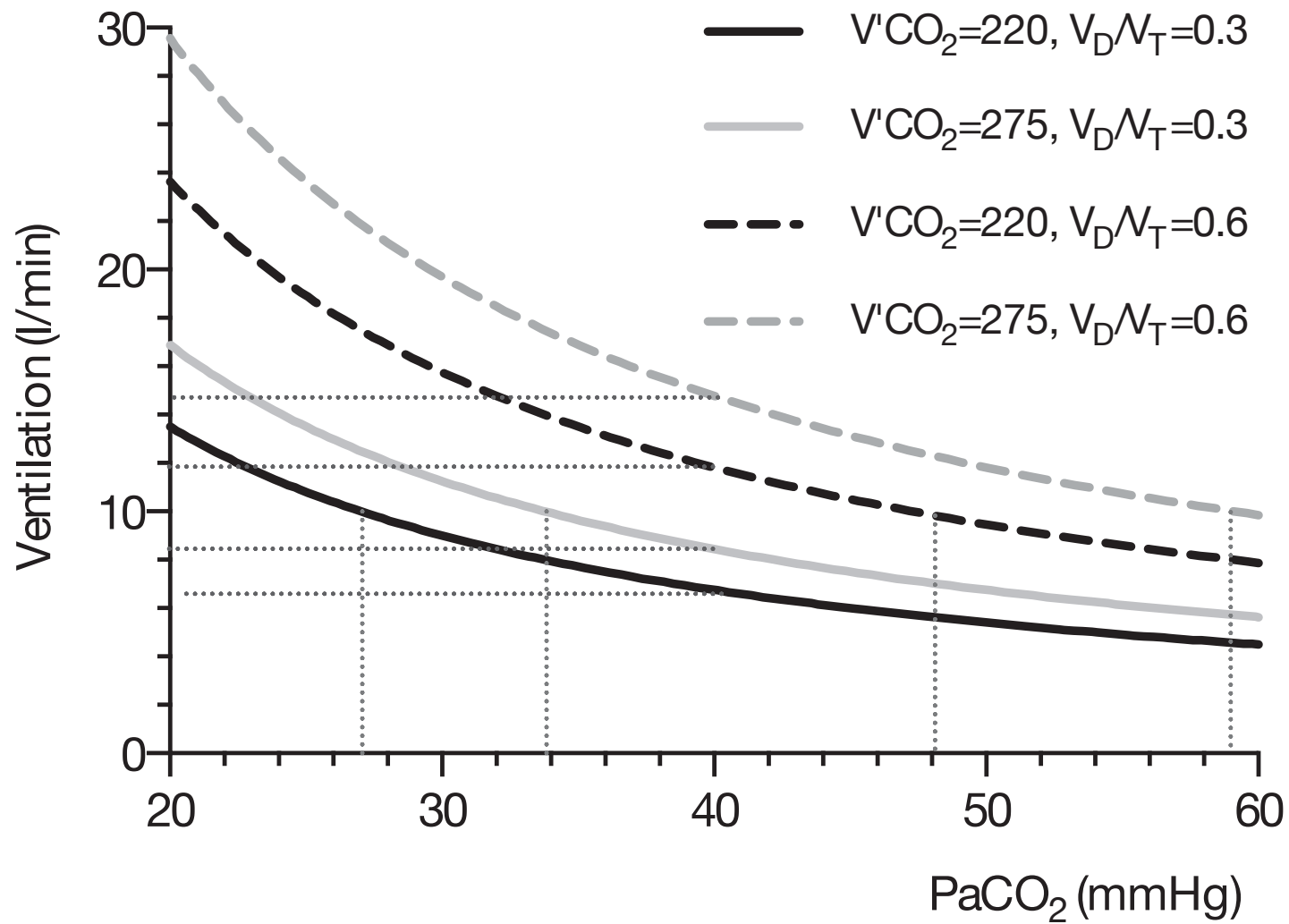


Figure 5

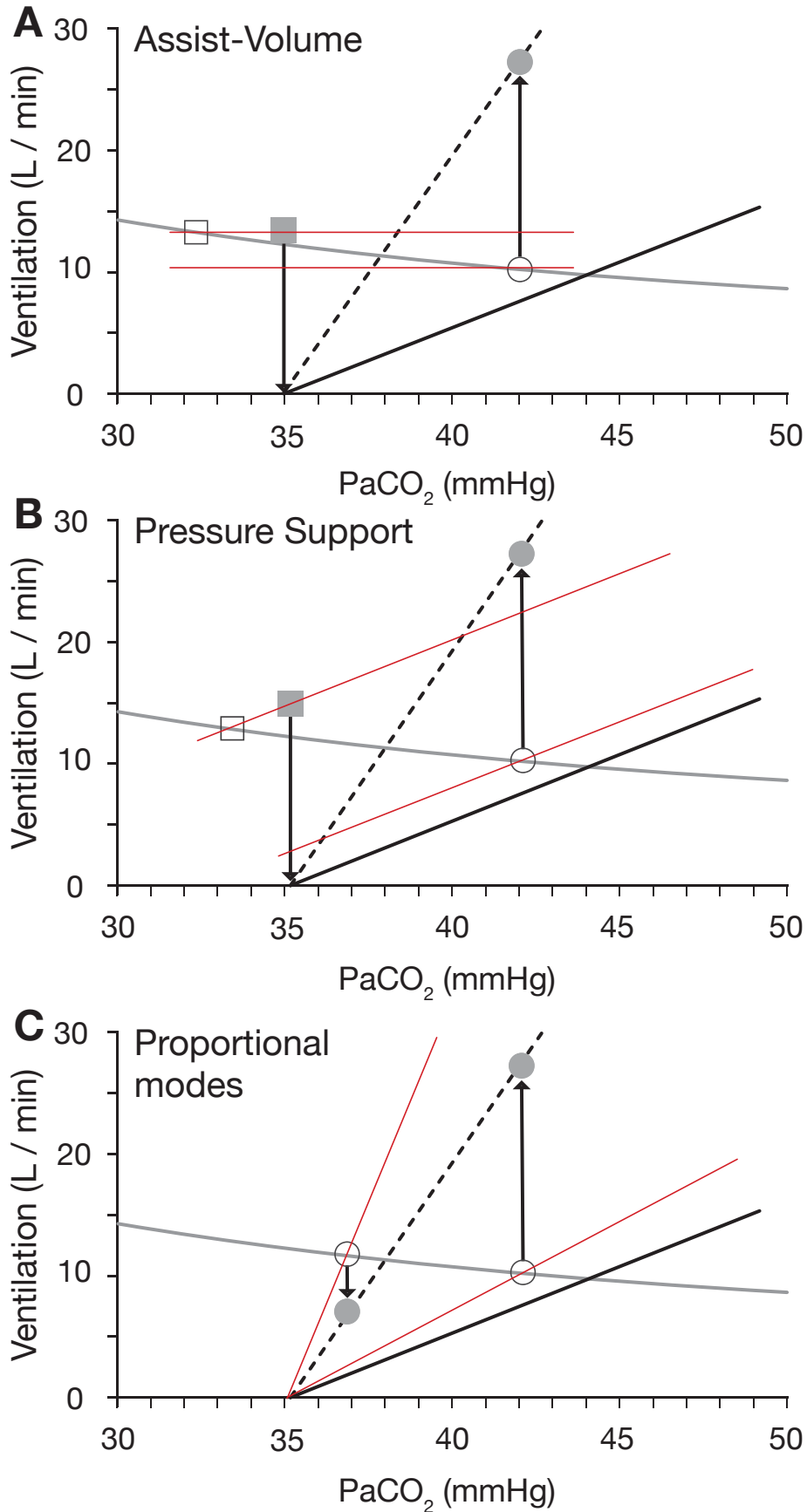


Figure 6

## On line data supplement

### Respiratory Drive in Critically Ill Patients: Pathophysiology and Clinical Implications

Katerina Vaporidi<sup>1</sup>, Evangelia Akoumianaki<sup>1</sup>, Irene Telias<sup>2,3</sup>, Ewan C. Goligher<sup>2,4,5</sup>,  
Laurent Brochard<sup>2,3\*</sup>, Dimitris Georgopoulos<sup>1\*</sup>.

<sup>1</sup>Department of Intensive Care Medicine, University Hospital of Heraklion, Medical School University of Crete, Greece. <sup>2</sup>Interdepartmental Division of Critical Care Medicine, University of Toronto, Toronto, Canada. <sup>3</sup>Keenan Research Center and Li Ka Shing Knowledge Institute, St. Michael's Hospital, Toronto, Canada. <sup>4</sup>Department of Medicine, University Health Network, Toronto, Canada. <sup>5</sup>Toronto General Hospital Research Institute, Toronto, Canada

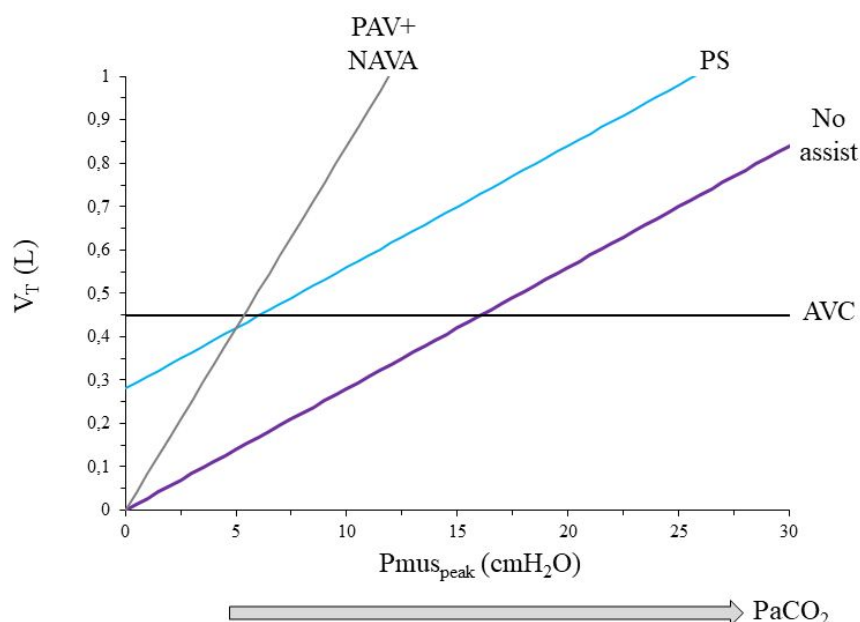
\*Equal contribution

Corresponding Author: D. Georgopoulos, Professor of Medicine,  
Director of Intensive Care Medicine Department,  
University Hospital of Heraklion, School of Medicine,  
University of Crete, Heraklion, Crete, Greece  
e-mail: [georgopd@uoc.gr](mailto:georgopd@uoc.gr)  
Phone: +306944727501

## Effects of assisted mechanical ventilation on respiratory drive

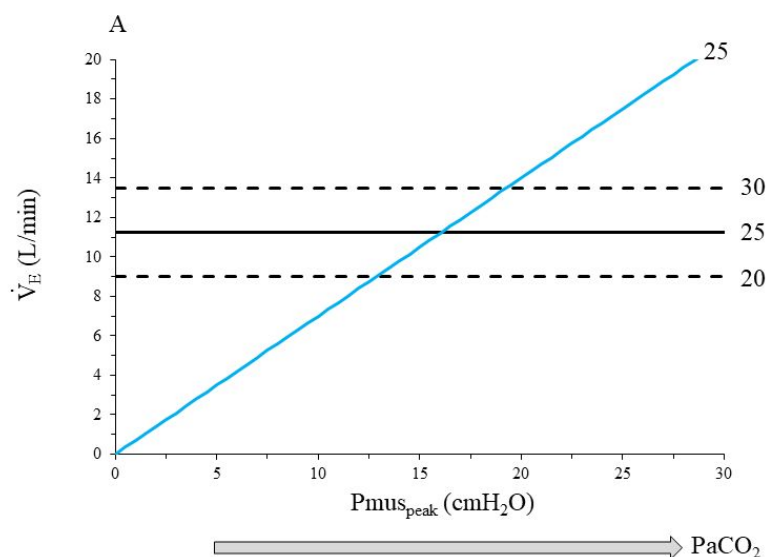
To understand how mechanical ventilation affects the respiratory drive it is crucial to recognize the relationships between 1) peak inspiratory muscle pressure per breath ( $P_{mus\_peak}$ ) and tidal volume ( $V_T$ ), and 2)  $P_{mus\_peak}$  and minute ventilation ( $V'_E$ ) during un-assisted and assisted breathing. It is also essential to realize that because  $P_{mus\_peak}$  increases linearly with increasing  $PaCO_2$  (1-4), these relationships are qualitatively similar to  $PaCO_2-V_T$  and  $PaCO_2-V'_E$ . During assisted breathing three modes of mechanical ventilation will be examined, a) assist volume control (AVC), b) pressure support (PS) and c) proportional assist (PAV+/NAVA). With AVC no back-up rate will be applied (back-up rate zero).

**Figure E1:  $P_{mus\_peak}-V_T$  relationship**

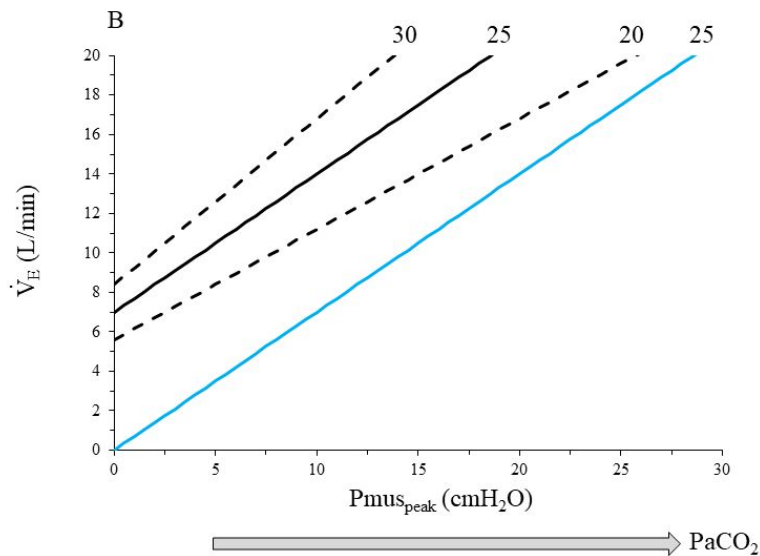


Relationship between  $P_{mus\_peak}$  (mainly determined by the respiratory drive) and  $V_T$  at constant respiratory system mechanics (elastance and resistance of respiratory system) and end-

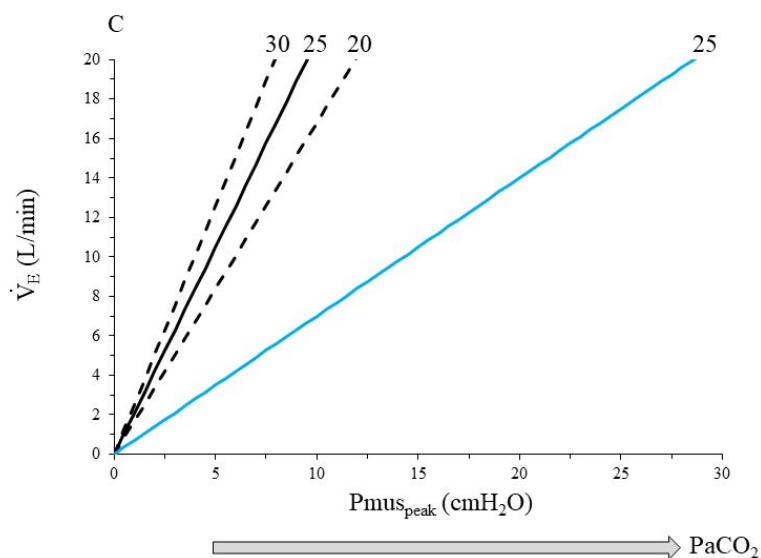
expiratory lung volume in: a) unassisted spontaneous breathing (purple line), b) AVC (black line), c) PS (blue line) and d) PAV+/NAVA (gray line). During un-assisted breathing the slope of the relationship depends exclusively on respiratory system mechanics. With AVC the slope is always zero (horizontal line), while with PS there is a parallel up-ward shift of the un-assisted breathing line without affecting the slope. With both modes changing the level of assist does not affect the slope but changes the position of the corresponding curve (parallel up-ward or down-ward movements, not shown). Notice that with both modes even at very low  $P_{mus_{peak}}$  (i.e. the patient relaxes all inspiratory muscles immediately after triggering due to low respiratory drive)  $V_T$ , depending on the level of assist, may be substantial. Compared to un-assisted breathing, proportional modes (PAV+/NAVA) increase the slope of  $P_{mus_{peak}}-V_T$  relationship depending on the level of assist. With PAV+/NAVA relaxation of inspiratory muscles immediately after triggering terminates the ventilator pressure and thus, even at very high assist (i.e. slope may approach 90° degrees),  $V_T$  is zero or very close to zero. Because  $P_{mus_{peak}}$  increases linearly with increasing  $PaCO_2$  (gray thick arrow),  $P_{mus_{peak}}-V_T$  relationship is qualitatively similar to  $PaCO_2-V_T$ .

**Figure E2:  $P_{\text{mus}_{\text{peak}}}$ - $V'_E$  relationship**

A: Relationship between  $P_{\text{mus}_{\text{peak}}}$  and  $V'_E$  during unassisted and assisted breathing with AVC. Respiratory system mechanics and end-expiratory lung volume are considered constant. The number beside each curve indicates respiratory rate (breaths/min). The blue continuous line denotes the  $P_{\text{mus}_{\text{peak}}}$ - $V'_E$  relationship during unassisted breathing. With AVC,  $V'_E$  at zero  $P_{\text{mus}_{\text{peak}}}$  represents  $V'_E$  when the patient relaxes all inspiratory muscles immediately after triggering (minimum  $V'_E$ ). With AVC at a respiratory rate similar to spontaneous breathing, the slope of the  $P_{\text{mus}_{\text{peak}}}$ - $V'_E$  relationship is zero (black continuous line). Increases and decreases of respiratory rate at the same assist level, move the relationship upwards and downwards (black dashed lines), respectively, while the slope remains zero. Because  $P_{\text{mus}_{\text{peak}}}$  increases linearly with increasing  $\text{PaCO}_2$  (gray thick arrow),  $P_{\text{mus}_{\text{peak}}}$ - $V'_E$  relationship is qualitatively similar to  $\text{PaCO}_2$ - $V'_E$ .



B: Relationship between  $P_{mus\_peak}$  and  $\dot{V}'_E$  during unassisted and assisted breathing with PS. Respiratory system mechanics and end-expiratory lung volume are considered constant. The number beside each curve indicates respiratory rate (breaths/min). The blue continuous line denotes the  $P_{mus\_peak}$ - $\dot{V}'_E$  relationship during unassisted breathing. With PS,  $\dot{V}'_E$  at zero  $P_{mus\_peak}$  represents  $\dot{V}'_E$  when the patient relaxes all inspiratory muscles immediately after triggering (minimum  $\dot{V}'_E$ ). At a respiratory rate similar to that during unassisted breathing, PS shifts the  $P_{mus\_peak}$ - $\dot{V}'_E$  relationship parallel upwards (black continuous line) with a slope identical to the slope of the corresponding relationship during unassisted breathing. An increase of the respiratory rate at the same level of assist will move the relationship upwards (higher minimum  $\dot{V}'_E$ ) and increase its slope, while a decrease will move the relationship downwards (lower minimum  $\dot{V}'_E$ ) and decrease its slope (black dashed lines). Because  $P_{mus\_peak}$  increases linearly with increasing  $PaCO_2$  (gray thick arrow),  $P_{mus\_peak}$ - $\dot{V}'_E$  relationship is qualitatively similar to  $PaCO_2$ - $\dot{V}'_E$ .



C: Relationship between  $P_{mus\_peak}$  and  $\dot{V}'_E$  during unassisted and assisted breathing with PAV+/NAVA. Respiratory system mechanics and end-expiratory lung volume are considered constant. The number beside each curve indicates respiratory rate (breaths/min). The blue continuous line denotes the  $P_{mus\_peak}$ - $\dot{V}'_E$  relationship during unassisted breathing. At a respiratory rate similar to that during unassisted breathing, PAV+/NAVA increase the slope of the  $P_{mus\_peak}$ - $\dot{V}'_E$  relationship (black solid line). At the same assist level, this slope will be increased or decreased if respiratory rate increases or decreases, respectively (black dashed lines). Of note, with PAV+/NAVA minimum  $\dot{V}'_E$  is always zero, irrespective of the level of assist (not shown) and respiratory rate. Because  $P_{mus\_peak}$  increases linearly with increasing  $PaCO_2$  (gray thick arrow),  $P_{mus\_peak}$ - $\dot{V}'_E$  relationship is qualitatively similar to  $PaCO_2$ - $\dot{V}'_E$ .

## Mechanical ventilation and respiratory drive

In the following examples (Fig. E3-E6) a simplified analysis highlights the effects of assisted mechanical ventilation on respiratory drive in a patient with impaired respiratory system mechanics. The brain and ventilation curves, and the relationships between  $\text{PaCO}_2$  and  $V'_E$  are presented for the three main modes of assisted mechanical ventilation, AVC, PS and PAV+/NAVA. In each mode four levels of assist are applied. A dead space per breath ( $V_D$ ) to  $V_T$  ratio ( $V_D/V_T$ ) of 0.5 and  $\text{CO}_2$  production ( $V'\text{CO}_2$ ) of 250 ml/min are used to construct the metabolic hyperbola (gray continuous line) as follows:

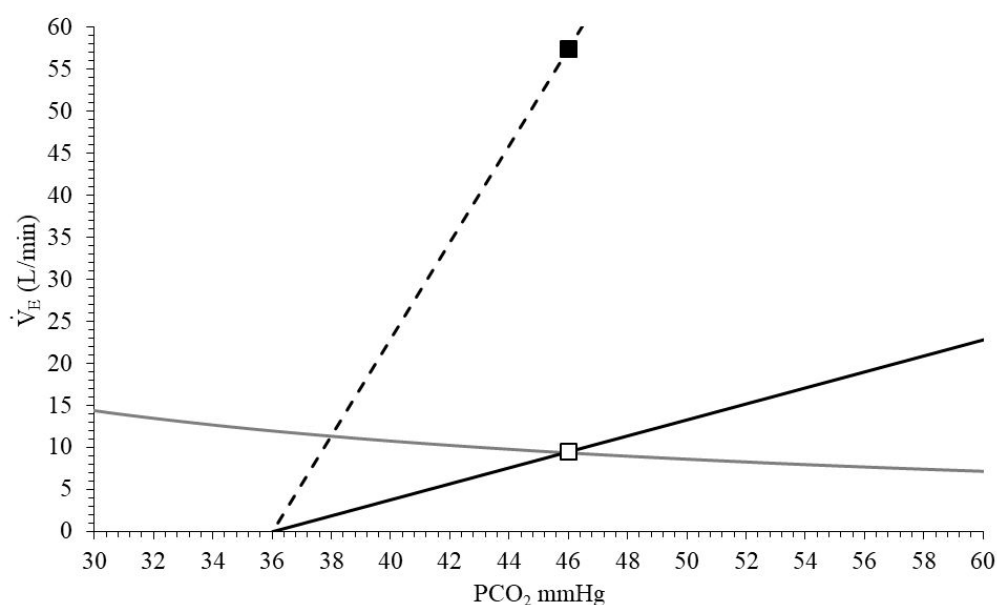
$$\text{PaCO}_2 = 0.863 * V'\text{CO}_2 / [V'_E * (1 - V_D/V_T)], \text{ Eq. 1.}$$

For simplicity, the metabolic hyperbola is considered constant with and without mechanical ventilation. In reality mechanical ventilation may change both  $V'\text{CO}_2$  (by altering the work of breathing) and  $V_D/V_T$ , and thus shift the metabolic hyperbola downward or upward.

The slope of the brain curve (black dashed line), representing the sensitivity to  $\text{CO}_2$  or the ventilatory demands at a given  $\text{PaCO}_2$ , is set at 5.75 l/min/mmHg. A relatively high slope is used (normal range 2-8 l/min/mmHg), to account for conditions commonly present in critically ill patients such as metabolic acidosis, stimulation of lung and chest wall receptors, or sepsis. The slope of the un-assisted ventilation curve (black continuous line) is set at 0.95 l/min/mmHg, to account for the derangement in respiratory system mechanics (i.e. high respiratory system elastance,  $E_{rs}$ ). The patient is considered to be sedated and an apneic threshold is set at  $\text{PaCO}_2$  of 36 mmHg. The same brain and un-assisted ventilation curves are used in all examples. Also, for simplicity it is assumed that a) all patient efforts trigger the ventilator (no ineffective efforts), b) end-expiratory lung volume is constant and c) respiratory rate remains the same between un-assisted and assisted breathing. The later assumption is valid, since respiratory rate may change minimally with mechanical ventilation and the level of assist, particularly at low and moderate levels of respiratory drive. See also Figure E2 (A-C) for the effect of a change in respiratory rate on the ventilation curve.

In this example respiratory rate of 25 breaths/min is applied and assuming a ratio of inspiratory to total breath duration ( $T_I/T_{TOT}$ ) of 0.3, inspiratory time of 0.72 sec is derived. At a given  $PaCO_2$  the respiratory drive is quantified as the tidal volume  $V_{Tbrain}$  desired by the respiratory center to inspiratory time ( $T_I$ ).  $V_{Tbrain}$  is calculated by dividing the ventilatory demands, as dictated by the brain curve at the given  $PaCO_2$  ( $V'_{Ebrain}$ ), with the respiratory rate (25 br/min), used in the example:  $V_{Tbrain} = V'_{Ebrain} / 25$ .

**Figure E3: Un-assisted breathing**



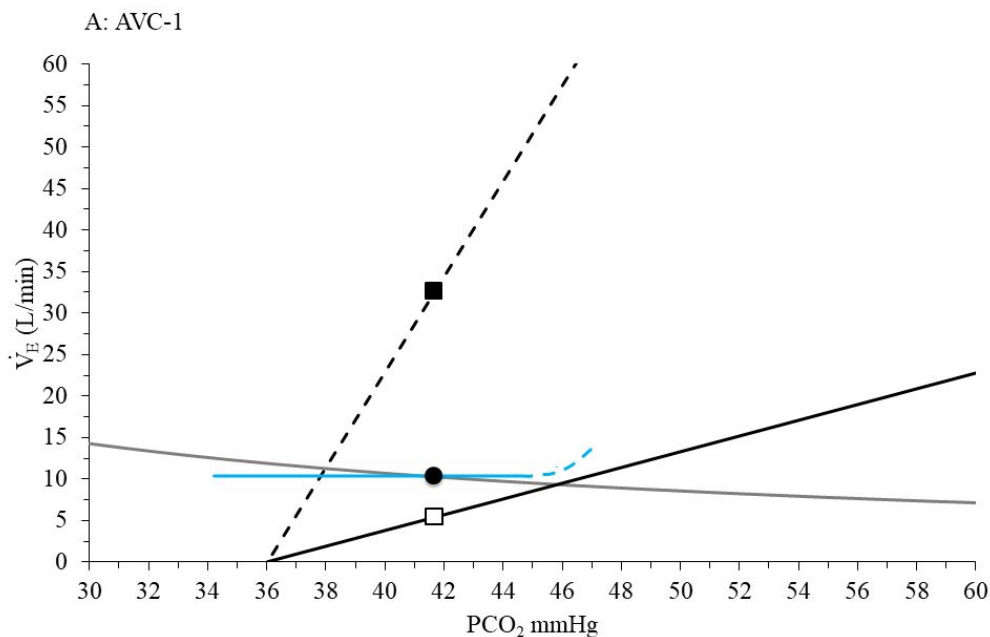
Relationships between  $PaCO_2$  and  $V'_E$  during un-assisted breathing. The  $PaCO_2$  desired by the brain is 38 mmHg (intersection between metabolic hyperbola and brain curve), while the actual  $PaCO_2$  is 46 mmHg (intersection between un-assisted ventilation curve and metabolic hyperbola, open square). At a  $PaCO_2$  of 46 mmHg the respiratory center demands 57.5 l/min of ventilation ( $V'_{Ebrain}$ , black square) as dictated by the brain curve, while actual  $V'_E$  is 9.4 l/min (open square). At this  $V'_{Ebrain}$  the desired  $V_T$  ( $V_{Tbrain}$ ) is 2.3 l (57.5/25) and respiratory drive ( $V_{Tbrain}/T_I$ ) is 3.2 l/sec (2.3/0.72). During un-assisted breathing this respiratory drive is similar to that obtained at moderate exercise. The ventilatory demands ( $V'_{Ebrain}=57.5$

l/min) are not met (actual  $V'_E=9.4$  l/min). The magnitude of unmet demands depends on  $PaCO_2$  and the slopes of brain and ventilator curves.

### Figure E4 – Assist Volume Control (no back-up rate)

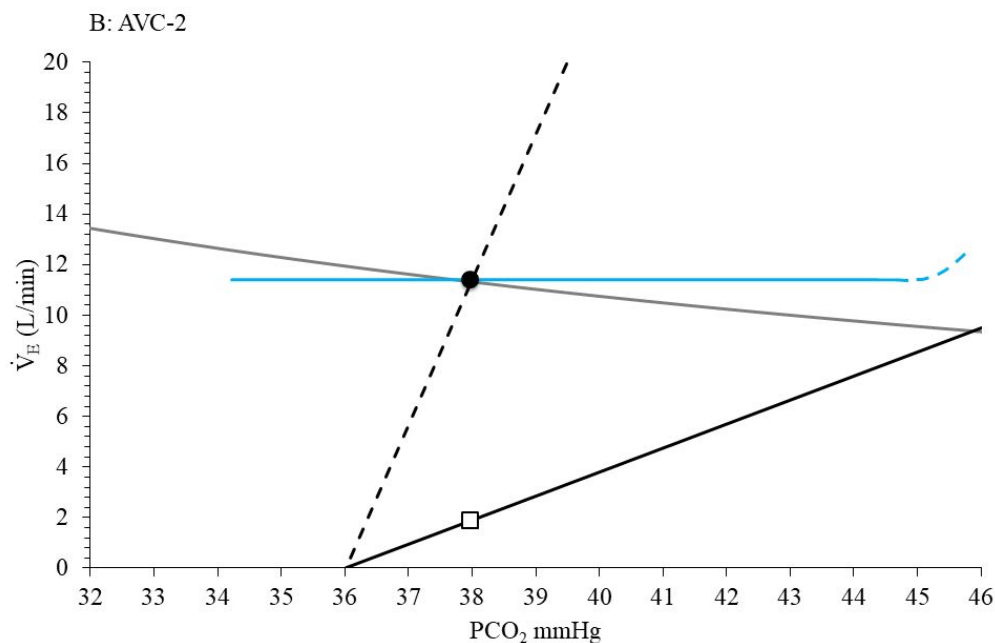
Relationships between  $PaCO_2$  and minute ventilation during different levels of AVC (A-D, from low to high assist). With AVC  $V_T$  is preset so un-assisted ventilation curve is shifted up-ward and its slope becomes zero (horizontal to  $PaCO_2$  axis) over a wide range of  $PaCO_2$  (blue continuous line). Notice that at high  $PaCO_2$  ventilation may increase due to progressive increase of patient respiratory rate, a common response pattern when  $V_T$  is constrained (blue dashed line).

For clarity of presentation the scale is increased in Figures 3B, 3C and 3D.

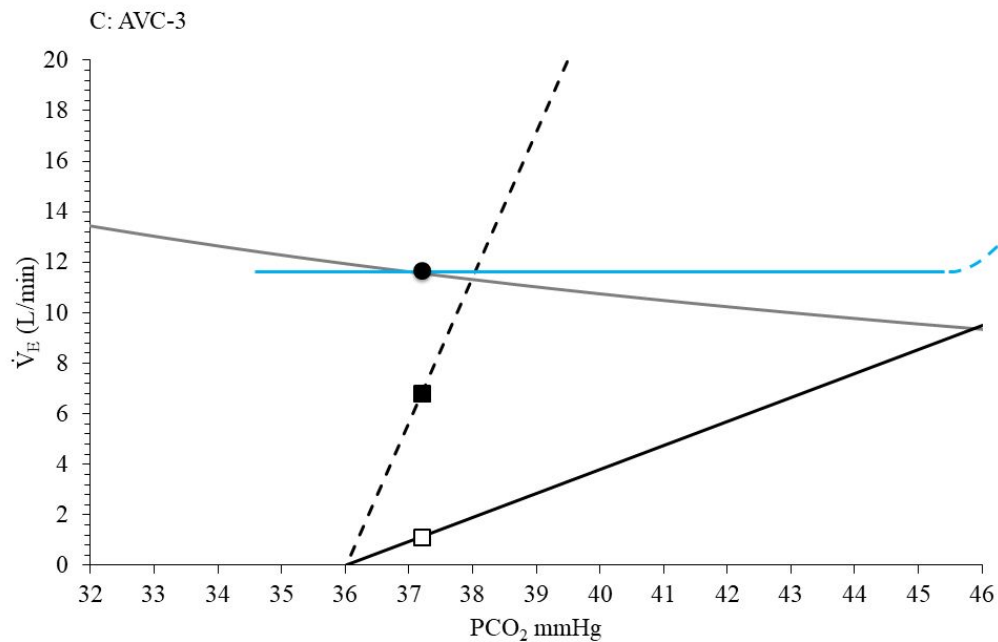


A: With AVC-1  $PaCO_2$  (black circle, intersection between the new ventilation curve and metabolic hyperbola) is 41.7 mmHg. Now, at a  $PaCO_2$  of 41.7 mmHg the respiratory center (brain curve) demands 32.8 l/min of ventilation ( $V'_{E_{brain}}$ , black square) which corresponds to  $V_{T_{brain}}$  of 1.31 l (32.8/25) and respiratory drive ( $V_{T_{brain}}/T_I$ ) of 1.82 l/sec. Yet, the actual  $V'_E$  is

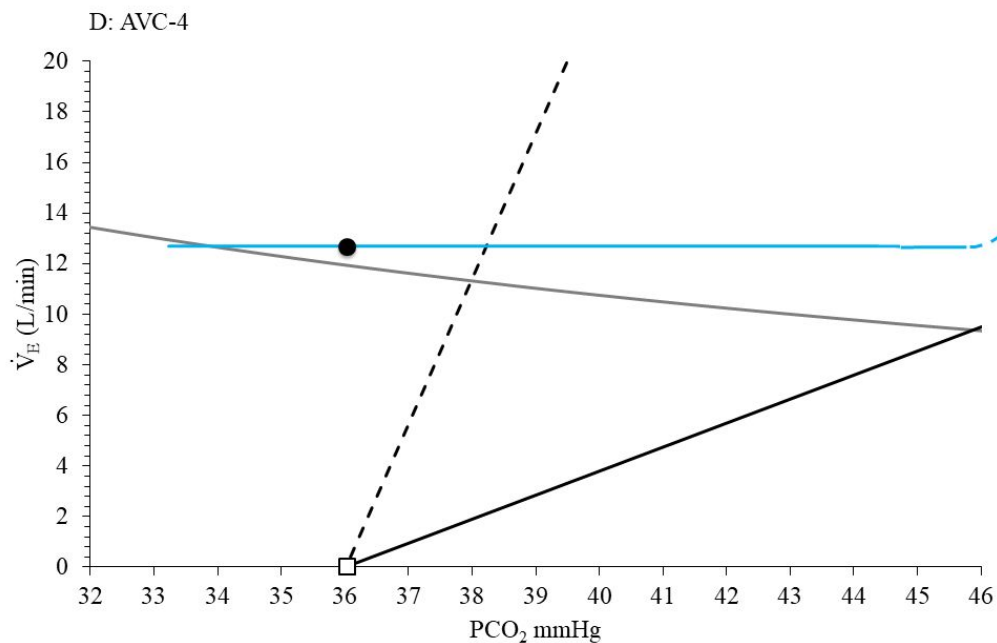
10.4 l/min (black circle). To achieve 10.4 l/min the patient contributes 5.4 l/min (open square, un-assisted ventilation curve) and the ventilator 5 l/min. The unmet demands are 22.4 l/min, due to dissociation between brain (black dashed line) and ventilation curve with AVC-1 (blue continuous line). Compared to un-assisted breathing AVC-1 decreases respiratory drive by 43% (from 3.2 l/sec to 1.82 l/sec).



B: With AVC-2 PaCO<sub>2</sub> (black circle, intersection point between the new ventilation curve and metabolic hyperbola) is 38 mmHg. Now, by chance, the intersection between the new ventilation curve and metabolic hyperbola is similar to that between brain curve and metabolic hyperbola. At PaCO<sub>2</sub> of 38 mmHg the respiratory center demands 11.4 l/min of ventilation. Since the actual PaCO<sub>2</sub> is similar to that desired by the respiratory center, the ventilatory demands are met by the delivered ventilation and V<sub>Tbrain</sub> equals the actual V<sub>T</sub> (0.46 l). The respiratory drive is 0.63 l/sec and is satisfied by actual V<sub>T</sub>/T<sub>I</sub> (mean inspiratory flow). To achieve 11.4 l/min the patient contributes 1.9 l/min (open square, un-assisted ventilation curve) and the ventilator 9.5 l/min. Compared to un-assisted breathing AVC-2 decreases respiratory drive by 80% (from 3.2 l/sec to 0.63 l/sec).



C: With AVC-3 PaCO<sub>2</sub> (black circle, intersection point between the new ventilation curve and metabolic hyperbola) is 37.2 mmHg, lower than that desired by the brain. At PaCO<sub>2</sub> of 37.2 mmHg the respiratory center demands 6.9 l/min of ventilation (black square),  $V_{T_{\text{brain}}}$  is 0.28 l and the respiratory drive ( $V_{T_{\text{brain}}}/T_i$ ) is 0.38 l/sec. Actual ventilation is 11.6 l/min. To achieve 11.6 l/min the patient contributes 1.1 l/min (open square, un-assisted ventilation curve) and the ventilator 10.5 l/min. Compared to un-assisted breathing AVC-3 decreases respiratory drive by 88% (from 3.2 l/sec to 0.38 l/sec).

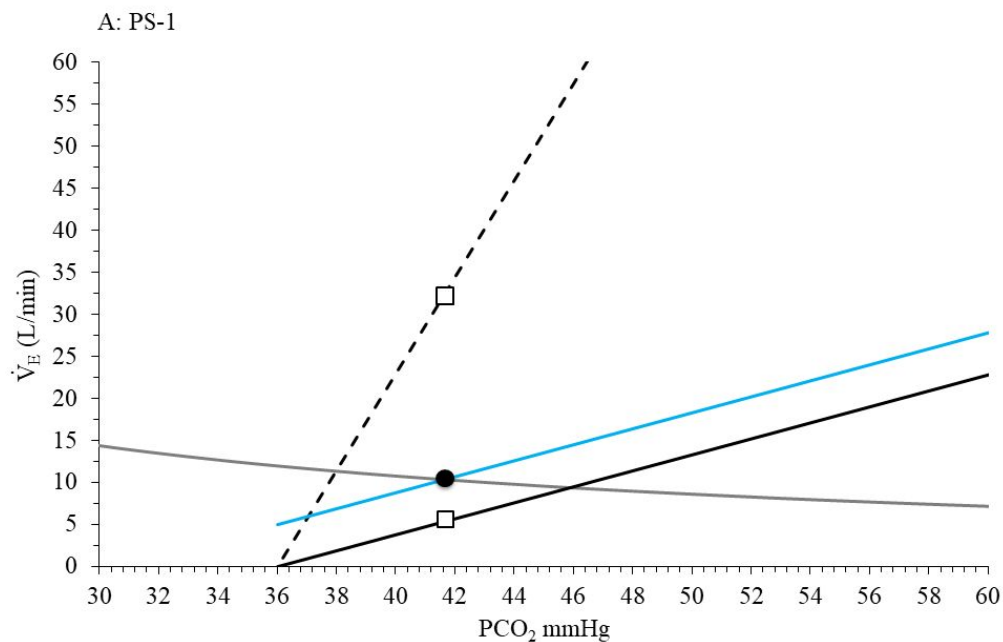


D: Although with AVC-4 the new ventilation curve (blue continuous line) intersects the metabolic hyperbola at PaCO<sub>2</sub> of 34 mmHg, the actual PaCO<sub>2</sub> is around 36 mmHg (black circle). Steady-state cannot be achieved because the occurrence of apneas prevents the PaCO<sub>2</sub> to drop below 36 mmHg (apneic threshold). At PaCO<sub>2</sub> of 36 mmHg respiratory center's output is zero (open square) and the patient exhibits periodic breathing. Respiratory drive hovers around zero (no steady-state). When the patient relaxes the diaphragm immediately after triggering (i.e. when between apneas respiratory drive is slightly above zero), the ventilator provides passively approximately 13.5 l/min (black circle). Ventilation ranges between zero (apnea) and approximately 13.5 l/min. Because inspiration is passive the patient is at risk of diaphragmatic atrophy.

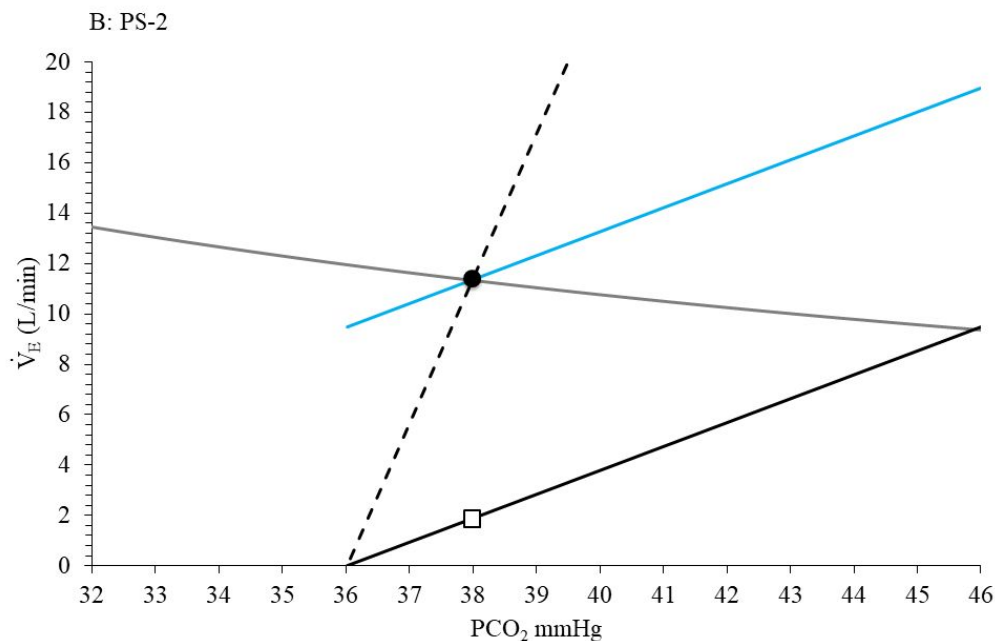
### Figure E5 – Pressure Support

Relationships between  $\text{PaCO}_2$  and minute ventilation during different levels of PS (A-D, from low to high PS). At constant respiratory rate, PS causes a parallel up-ward deviation of the un-assisted ventilation curve. The magnitude of the deviation depends on PS level, mechanics of respiratory system, rising time and cycling off criterion.

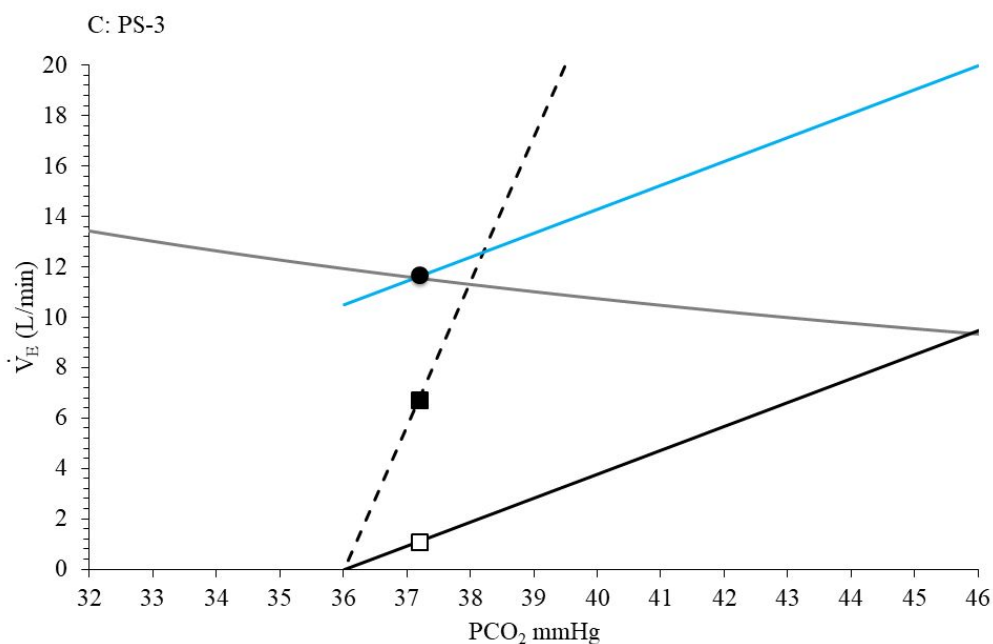
For clarity of presentation the scale is increased in Figures E5B, E5C and E5D.



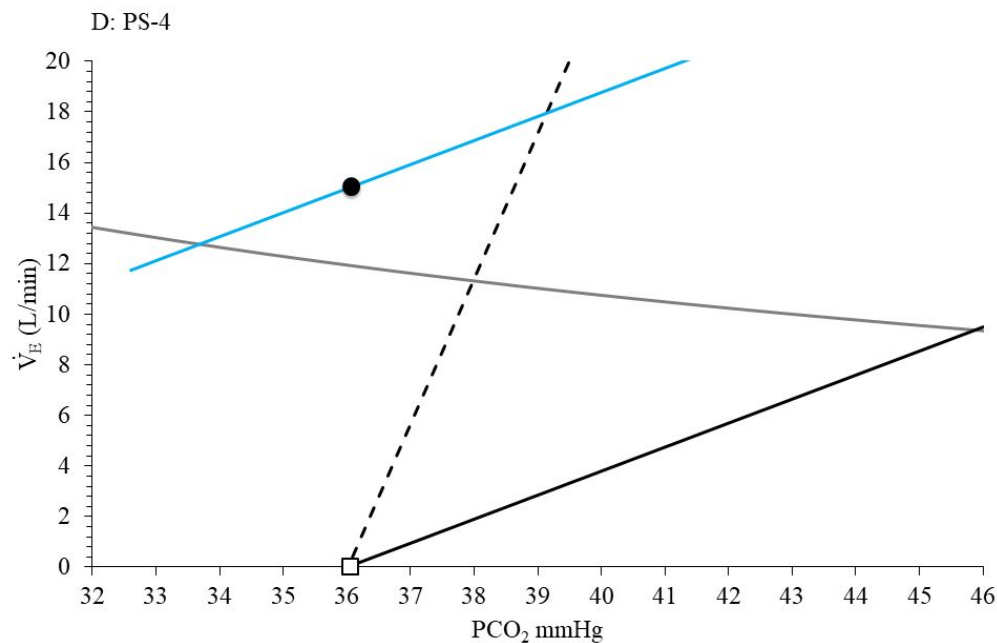
A: With PS-1  $\text{PaCO}_2$  (black circle, intersection between the new ventilation curve and metabolic hyperbola) is 41.7 mmHg. Now, at a  $\text{PaCO}_2$  of 41.7 mmHg the respiratory center (brain curve) demands 32.8 l/min of ventilation ( $V_{E\text{brain}}$ , black square) which corresponds to  $V_{T\text{brain}}$  of 1.31 l (32.8/25) and respiratory drive ( $V_{T\text{brain}}/T_I$ ) of 1.82 l/sec. Yet, the actual  $V'_E$  is 10.4 l/min (black circle). To achieve 10.4 l/min the patient contributes 5.4 l/min (open square, un-assisted ventilation curve) and the ventilator 5 l/min. The unmet demands are 22.4 l/min, due to dissociation between brain (black dashed line) and ventilation curve with PS-1 (blue continuous line). Compared to un-assisted breathing PS-1 decreases respiratory drive by 43% (from 3.2 l/sec to 1.82 l/sec).



B: With PS-2 PaCO<sub>2</sub> (black circle, intersection point between the new ventilation curve and metabolic hyperbola) is 38 mmHg. Now, by chance, the intersection between the new ventilation curve and metabolic hyperbola is similar to that between brain curve and metabolic hyperbola. At PaCO<sub>2</sub> of 38 mmHg the respiratory center demands 11.4 l/min of ventilation. Since the actual PaCO<sub>2</sub> is similar to that desired by the respiratory center, the ventilatory demands are met by the delivered ventilation and V<sub>Tbrain</sub> equals the actual V<sub>T</sub> (0.46 l). The respiratory drive is 0.63 l/sec and is satisfied by actual V<sub>T</sub>/T<sub>I</sub> (mean inspiratory flow). To achieve 11.4 l/min the patient contributes 1.9 l/min (open square, un-assisted ventilation curve) and the ventilator 9.5 l/min. Compared to un-assisted breathing PS-2 decreases respiratory drive by 80% (from 3.2 l/sec to 0.63 l/sec).



C: With PS-3 PaCO<sub>2</sub> (black circle, intersection point between the new ventilation curve and metabolic hyperbola) is 37.2 mmHg, lower than that desired by the brain. At PaCO<sub>2</sub> of 37.2 mmHg the respiratory center demands 6.9 l/min of ventilation (black square),  $V_{T_{\text{brain}}}$  is 0.28 l and the respiratory drive ( $V_{T_{\text{brain}}}/T_i$ ) is 0.38 l/sec. Actual ventilation is 11.6 l/min. To achieve 11.6 l/min the patient contributes 1.1 l/min (open square, un-assisted ventilation curve) and the ventilator 10.5 l/min. Compared to un-assisted breathing PS-3 decreases respiratory drive by 88% (from 3.2 l/sec to 0.38 l/sec).

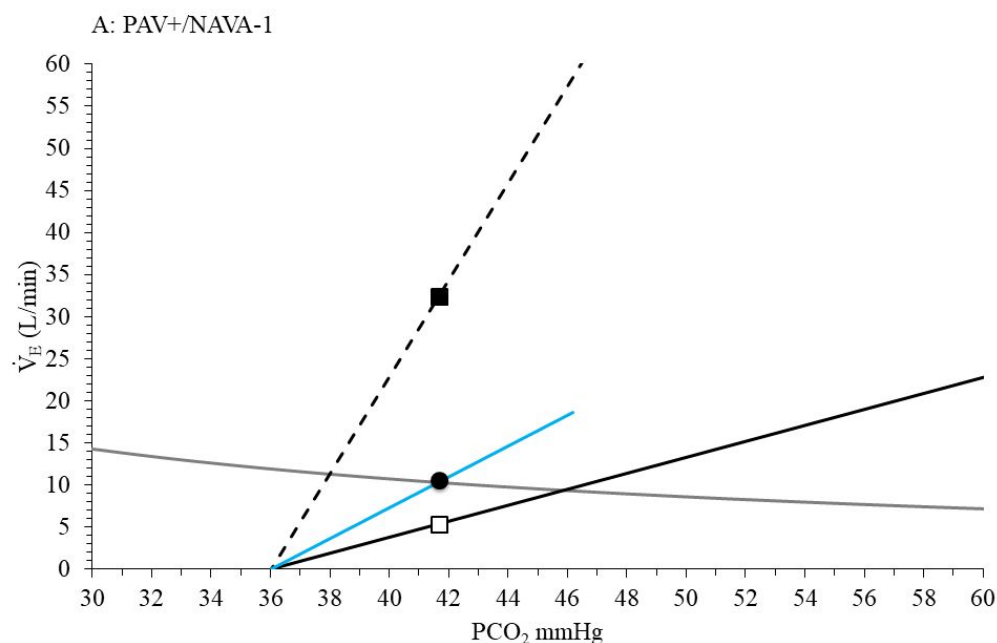


D: Although with PS-4 the new ventilation curve (blue line) intersects the metabolic hyperbola at PaCO<sub>2</sub> of 33.8 mmHg, the actual PaCO<sub>2</sub> is around 36 mmHg (black circle). Steady-state cannot be achieved because the occurrence of apneas prevents the PaCO<sub>2</sub> to drop below 36 mmHg (apneic threshold). At PaCO<sub>2</sub> of 36 mmHg respiratory center's output is zero (open square) and the patient exhibits periodic breathing. Respiratory drive hovers around zero (no steady-state). When the patient relaxes the diaphragm immediately after triggering (i.e. when, between apneas, the respiratory drive is slightly above zero), the ventilator provides passively approximately 14.5 l/min (black circle). Ventilation ranges between zero (apnea) and approximately 14.5 l/min. Because inspiration is passive the patient is at risk of diaphragmatic atrophy. Compared to AVC-4, with PS-4 apneas will last longer due to higher ventilation when the patient triggers the ventilator.

### Figure E6 – Proportional modes

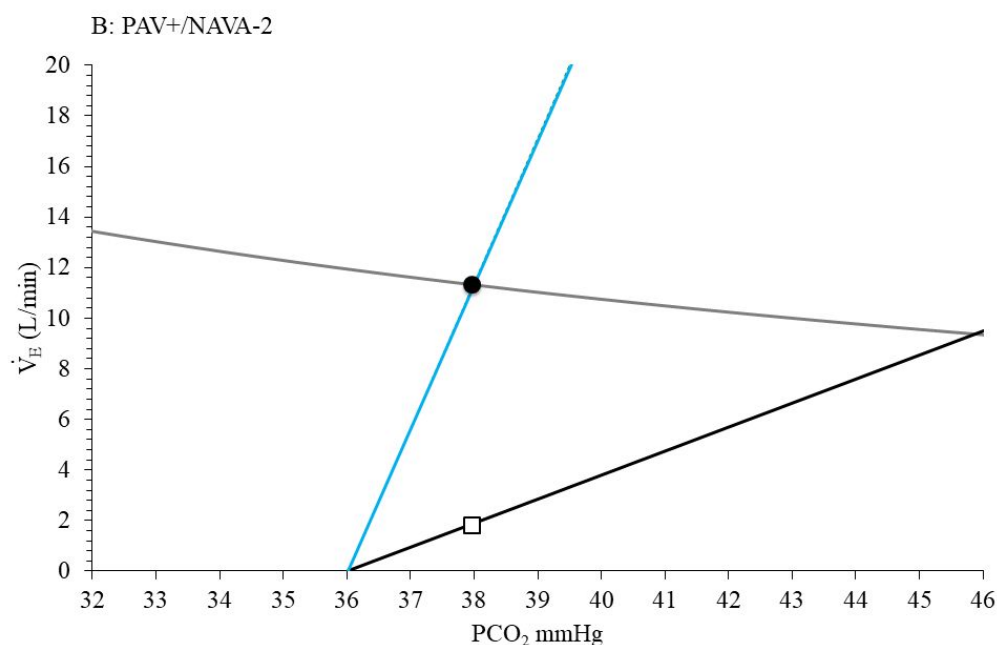
Relationships between  $\text{PaCO}_2$  and minute ventilation during different levels of PAV+/NAVA (A-D, from low to high assist). At constant respiratory rate, PAV+/NAVA increases the slope of un-assisted ventilation curve. The starting point of the ventilation curve with PAV+/NAVA is similar to that of un-assisted ventilation curve ( $\text{PaCO}_2$  36 mmHg, apneic threshold). The slope of the assisted ventilation curve depends on respiratory system mechanics and level of assist.

For clarity of presentation the scale is increased in Figures E6B, E6C and E6D.

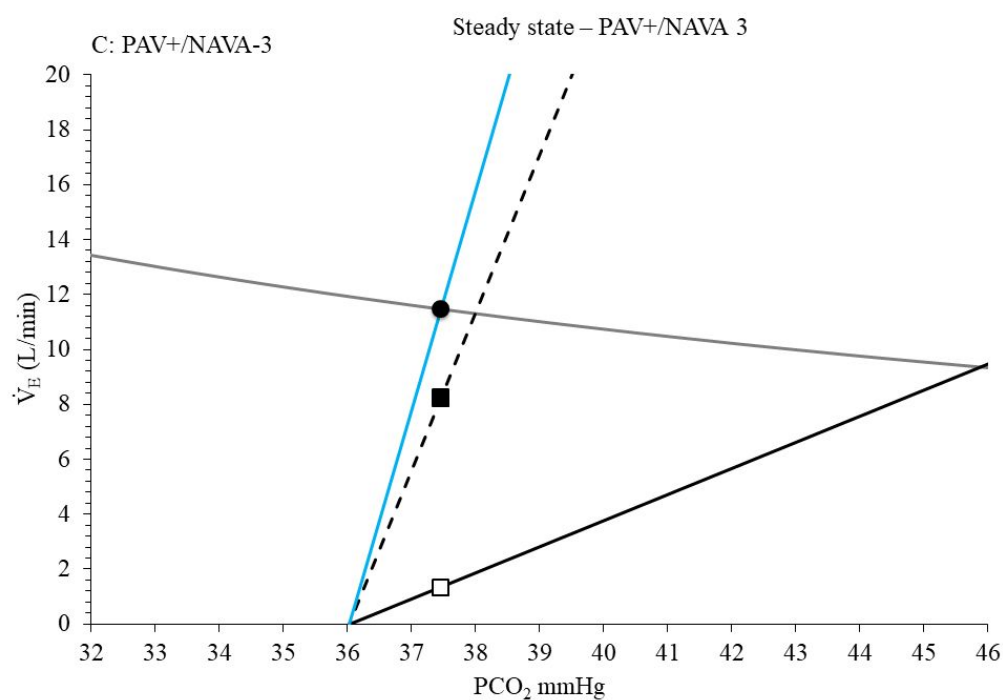


A: With PAV+/NAVA-1  $\text{PaCO}_2$  (black circle, intersection between the new ventilation curve and metabolic hyperbola) is 41.7 mmHg. Now, at a  $\text{PaCO}_2$  of 41.7 mmHg the respiratory center (brain curve) demands 32.8 l/min of ventilation ( $V'_{E\text{brain}}$ , black square) which corresponds to  $V_{T\text{brain}}$  of 1.31 l (32.8/25) and respiratory drive ( $V_{T\text{brain}}/T_I$ ) of 1.82 l/sec. Yet, the actual  $V'_E$  is 10.4 l/min (black circle). To achieve 10.4 l/min the patient contributes 5.4 l/min (open square, un-assisted ventilation curve) and the ventilator 5 l/min. The unmet demands are 22.4 l/min, due to dissociation between brain (black dashed line) and ventilation curve

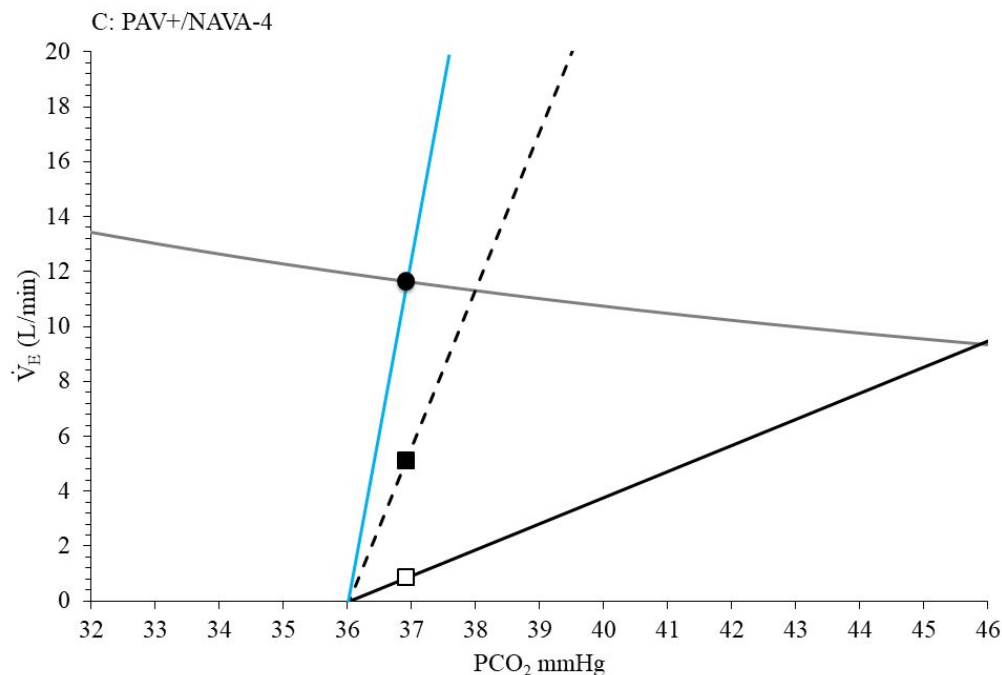
with PAV+/NAVA-1 (blue continuous line). Compared to un-assisted breathing PAV+/NAVA-1 decreases respiratory drive by 43% (from 3.2 l/sec to 1.82 l/sec).



B: With PAV+/NAVA-2 PaCO<sub>2</sub> (black circle, intersection point between the new ventilation curve and metabolic hyperbola) is 38 mmHg. Now, by chance, the intersection between the new ventilation curve and metabolic hyperbola is similar to that between brain curve and metabolic hyperbola. At PaCO<sub>2</sub> of 38 mmHg the respiratory center demands 11.4 l/min of ventilation. Since the actual PaCO<sub>2</sub> is similar to that desired by the respiratory center, the ventilatory demands are met by the delivered ventilation and V<sub>Tbrain</sub> equals the actual V<sub>T</sub> (0.46 l). The respiratory drive is 0.63 l/sec and is satisfied by actual V<sub>T</sub>/T<sub>I</sub> (mean inspiratory flow). To achieve 11.4 l/min the patient contributes 1.9 l/min (open square, un-assisted ventilation curve) and the ventilator 9.5 l/min. Compared to un-assisted breathing PAV+/NAVA-2 decreases respiratory drive by 80% (from 3.2 l/sec to 0.63 l/sec).



C: With PAV+/NAVA-3 PaCO<sub>2</sub> (black circle, intersection point between the new ventilation curve and metabolic hyperbola) is 37.4 mmHg, lower than that desired by the brain. At PaCO<sub>2</sub> of 37.2 mmHg the respiratory center demands 8.0 l/min of ventilation (black square),  $V_{T\text{brain}}$  is 0.32 l and the respiratory drive ( $V_{T\text{brain}}/T_I$ ) is 0.44 l/sec. Actual ventilation is 11.5 l/min. To achieve 11.5 l/min the patient contributes 1.0 l/min (open square, un-assisted ventilation curve) and the ventilator 10.5 l/min. Compared to un-assisted breathing PAV+/NAVA-3 decreases respiratory drive by 86% (from 3.2 l/sec to 0.44 l/sec).



D: With PAV+/NAVA-4 (highest possible assist at least with PAV+, amplification factor close to 10) PaCO<sub>2</sub> (black circle, intersection point between the new ventilation curve and metabolic hyperbola) is 36.9 mmHg, lower than that desired by the brain. At PaCO<sub>2</sub> of 36.9 mmHg the respiratory center demands 5.2 l/min of ventilation (black square),  $V_{T_{\text{brain}}}$  is 0.21 l and the respiratory drive ( $V_{T_{\text{brain}}}/T_I$ ) is 0.29 l/sec. Actual ventilation is 11.7 l/min. To achieve 11.7 l/min the patient contributes 0.86 l/min (open square, un-assisted ventilation curve) and the ventilator 10.8 l/min. Compared to un-assisted breathing PAV+/NAVA-4 decreases respiratory drive by 91% (from 3.2 l/sec to 0.29 l/sec). Contrary to PS and AVC, even at very high assist (slope of ventilation curve slightly lower than 90°) steady state is achieved.

## References

1. Clark FJ, von Euler C. On the regulation of depth and rate of breathing. *The Journal of physiology* 1972; 222: 267-295.
2. Duffin J, Mohan RM, Vasiliou P, Stephenson R, Mahamed S. A model of the chemoreflex control of breathing in humans: model parameters measurement. *Respiration physiology* 2000; 120: 13-26.
3. Georgopoulos D, Mitrouska I, Bshouty Z, Webster K, Patakas D, Younes M. Respiratory response to CO<sub>2</sub> during pressure-support ventilation in conscious normal humans. *American journal of respiratory and critical care medicine* 1997; 156: 146-154.
4. Georgopoulos D, Mitrouska I, Webster K, Bshouty Z, Younes M. Effects of inspiratory muscle unloading on the response of respiratory motor output to CO<sub>2</sub>. *American journal of respiratory and critical care medicine* 1997; 155: 2000-2009.